# SYNTHESIS, CHARACTERIZATION and APPLICATION of POLY(STYRENE- 4-VINYL PYRIDINE) MEMBRANES ASSEMBLED with SINGLE-WALL CARBON NANOTUBES

Thesis by

**Haoze He**

In Partial Fulfillment of the Requirements

For the Degree of

**Master of Science**

King Abdullah University of Science and Technology

Thuwal, Kingdom of Saudi Arabia

06/2011

The thesis of Haoze He is approved by the examination committee.

Committee Chairperson: Klaus-Viktor Peinemann

Committee Member: Suzana Nunes

Committee Member: Zhiping Lai

# ABSTRACT

## Synthesis, Characterization and Application of Poly(styrene- 4-vinyl pyridine) Membranes Assembled with Single-Wall Carbon Nanotubes

Haoze He

Poly(styrene-4-vinylpyridine) (PS-P4VP) isoporous membranes were prepared and their properties were evaluated in this research. The solution was prepared by dissolving PS-P4VP polymer with necessary additives into a 1:1:1 1,4-dioxane – N,N-dimethyl formamide – tetrahydrofuran (DOX-DMF-THF, DDT) solvent. Then 0.5-1.0 mL of the primary solution was cast onto the non-woven substrate membrane on a glass slide, evaporated for 15-20 sec and immersed into de-ionized water for more than 30 min for the solidification of isoporous structure and for the formation of the primary films, which could be post-processed in different ways for different tests. The membrane surface presents a well-ordered, hexagonal self-assembly structure, which is fit for aqueous and gaseous filtration. The pore size of the isoporous surface is 30~40 nm. The pore size is also sensitive to $[H^+]$ in the solution and a typical pair of S-shape pH-correlation curves with significant hysteresis was found. Four techniques were tried to improve the properties of the membranes in this research: 1) 1,4-diiodobutane was introduced to chemically change the structure as a cross-linking agent. 2) single-wall carbon nanotube (SWCNT) was linked to the membranes in order to strengthen the stability and

rigidity and to reduce the hysteresis. 3) Homo-poly(4-vinylpyridine) (homo-P4VP) was added and inserted into the PS-P4VP micelles to affect the pore size and surface structure. 4) Copper acetate ($Cu(Ac)_2$) was used as substitute of dioxane to prepare the $Cu(Ac)_2$-DMF-THF (CDT) mixed solvent, for a better SWCNT dispersion. All the possible improvements were judged by the atomic force microscopy (AFM) images, water and gas flux tests and pH-correlation curves. The introduction of SWCNT was the most important innovation in this research and is promising in future applications.

# ACKNOWLEDGEMENT

I would like to sincerely thank my supervisor Dr Klaus-Viktor Peinemann for his continuous guidance throughout my research and thesis work. His valuable suggestions and enthusiastic encouragement made my research very enjoyable and ultimately fruitful. I would also like to thank him for providing me with an excellent research environment.

In the Peinemann group, I would like to thank post-doc Mr Madhavan Karunakaran for his explanation of the self-assembly mechanism of diblock copolymer membranes; research scientist Mr Neelakanda Pradeep, for his illumination in the fucntion of single-wall carbon nanotube; graduate Ms Xu Zhao, for her instructuion on the chemical properties of reagents; and graduate Ms Eki Listya Rini, for her suggestions on the gas flux research work.

In KAUST Advanced Membrane and Porous Materials Center, I would like to thank Dr Ingo Pinnau, for his acceptance for me entering the center and using research facilities; and secretary Ms Melinda Leighton, for her help to make my research go smooth.

I would like to thank Dr Suzana Nunes for her successful instruction in the introductionary knowledge of polymers and macromolecules; and Dr Zhiping Lai, for his worthy suggestion in my thesis work.

I would like to thank my parents for their continuous encouragement during this journey and their deep moral support at all times. And I also would like to

thank my fiancee for her effective advice in my research as a chemistry graduate, and her hard work in the proofreading of this thesis.

Lastly, I would like to thank all the people at King Abdullah University of Science and Technology, Thuwal, Makkah, Saudi Arabia for their support through out my two-year precious life here.

# TABLE of CONTENTS

# LIST of ABBREVIATIONS

| | |
|---|---|
| PS-P4VP | poly(styrene-4-vinylpyridine) |
| GS | gas separation |
| homo-P4VP | homo-poly (4-vinylpyridine) |
| DOX | 1,4-dioxane |
| DMF | N,N-dimethyl formamide |
| THF | tetrahydrofuran |
| DDT | 1:1:1 wt% DOX-DMF-THF solvent |
| $Cu(Ac)_2$ | copper acetate |
| CDT | $Cu(Ac)_2$-DMF-THF solvent whose recipe is listed in Table 2.3.5 |
| HCl | hydrochloric acid |
| $N_2$ | nitrogen molecule / gas |
| $CO_2$ | carbon dioxide molecule / gas |
| SWCNT | single-wall carbon nanotube |
| AFM | atomic force microscopy |
| P# | catalog number of PS-P4VP products from Polymer Source™ |

# LIST of SYMBOLS

| | |
|---|---|
| $M_w$ | number average molecular weight |
| $M_n$ | weight average molecular weight |
| $C_x$ | concentration of solute x (wt% in this research) |
| V | solution volume |
| l | membrane thickness |
| t | time for solution to pass through the membrane in flux test |
| P | permeability |
| J or Q | permeance (or flux) |
| Δp | the pressure difference between feed and permeate |
| R | pore radius |
| ε | porosity |
| γ | viscosity |
| $k_B$ | Boltzman constant |
| r | pore radius |
| [A] | concentration of species A in aqueous solution |
| p | molecular packing parameter |
| $V_0$ | volume of the a polystyrene block |
| $a_0$ | optimal surface area of polystyrene block at the block interface |
| d | length of polystyrene block |

# LIST of ILLUSTRTIONS

# LIST of TABLES

# Chapter I

# INTRODUCTION

## 1. Membrane Technology in Mass Separations

Membrane technology is a powerful tool nowadays in solving some important global problems and in developing new industrial processes needed for a sustainable growth[1]. Two major fields of membrane technology are water purification and gas separation.

In water purification, membranes and their combinations with other systems have already become an effective method for satisfying freshwater demands at lower cost and minimum environmental impacts in many droughty areas of the world[1]. Theoretically, membrane filtration is a factor of 10 times more energetically efficient than thermal processes for water desalination[2]. The major production cycles consume 40-50% of the energy used just in separations carried out by inefficient thermally driven processes[1], while membranes supply an effective way to solve this problem.

Membrane gas separation (GS) is a pressure-driven process with different industrial applications. Since 1980s when the serial productions of commercial polymeric membranes were implemented, membrane GS had rapidly become a competitive separation technology[1]. During the past 20 years, sales of membrane

gas separation equipment have grown to a $150 million/year business[3].

### a) Membrane Processes in Water Purification

In recent years global water shortage has become one of the most serious crises. Many well-known worldwide problems are associated with the lacking of clean freshwater: 1.2 billion people lack access to safe drinking water, 2.6 billion have little or no sanitation, and millions die annually – 3,900 children a day – from diseases that are transmitted through water polluted by chemicals or human excreta[4].

Traditional chemical treatment of wastewater, before it was discharged in lakes and rivers, or post-processed in municipal ways for daily consumption, usually brought pollutants from one place to another, which was obviously not green or sustainable[5]. Later people started to use new techniques to avoid bringing in chemicals, such as photocatalytic process which allows in many cases a complete degradation of organic pollutants into small and harmless species[7]. However, this type of reaction requires special devices that are not financial feasible for a spread in industry.

Membrane separation technology is an economic and sustainable option. Due to the selectivity of membranes to given molecules/ions in adsorption, reaction and permeation, Membrane separation has already proved competitive with respect to other separation processes, concerning energy costs, material recovery, reduction of the environmental impact and achievement of integrated processes with selective

removal of some components[6,7,8].

Membranes can function by two transport mechanisms in water filtration: pore flow and solution diffusion, as depicted schematically in Fig 1.1.1[9,10,11]. The scale of water molecule is about 2nm, which is far less than 30~40nm, the pore size of poly(styrene-4-vinylpyridine) (PS-P4VP) isoporous membrane, which is the membrane of interest in this research. This fact indicates that its mechanism is pore-flow.

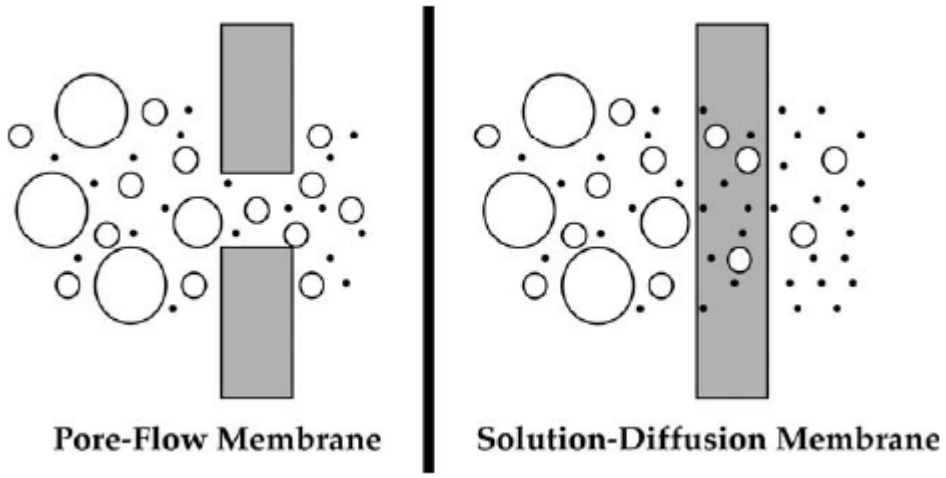


Fig 1.1.1 Pore-flow Membrane Transport and Solution-Diffusion Membrane Transport[11]

**b) Membrane Processes in Gas Separation**

The use of membranes in GS processes is growing at a slow but steady rate[12]. In 2002 Baker estimated the market scale of membrane GS technology in year 2020 to be four times more than that of year 2000[12]. It is expected that membrane GS will play an increasingly important role in reducing costs and environmental impacts of industrial processes[1], since the global energy and resources are being consumed

year by year.

More than 90% of this business involves the separation of non-condensable gases: nitrogen from air; carbon dioxide from methane; and hydrogen from nitrogen, argon, or methane[12]. There is still a large market potential for membrane-based GS technologies. Currently, eight or nine polymer materials have made at least 90% of the total installed gas separation membrane base in the market (Table 1.3.1).

Table 1.3.1 Principal Gas Separation Markets, Producers, and Membrane Systems (2000) [12]

| company | principal markets/ estimated annual sales | principal membrane material used | module type |
|---|---|---|---|
| Permea (Air Products) | large gas companies | polysulfone | hollow fiber |
| Medal (Air Liquide) | nitrogen/air ($75 million/year) | polyimide/polyaramide | |
| IMS (Praxair) | hydrogen separation ($25 million/year) | polyimide | |
| Generon (MG) | | tetrabromo polycarbonate | |
| GMS (Kvaerner) | mostly natural gas separations | cellulose acetate | spiral-wound |
| Separex (UOP) | carbon dioxide/methane | | |
| Cynara (Natco) | ($30 million/year) | | hollow fiber |
| Aquilo | vapor/gas separation, air dehydration, other ($20 million/year) | polyphenylene oxide | hollow fiber |
| Parker-Hannifin | | polyimide | |
| Ube | | | |
| GKSS Licensees | | silicone rubber | plate-and-frame |
| MTR | | | spiral-wound |

Actually, hundreds of new polymer materials have been reported to make advanced membrane within last several years, but the related technologies have not yet been mature in industry[12]. Permeability and selectivity are two most important criteria that must be satisfied for a proper industrial membrane[12], and therefore some potential disadvantages of new membrane materials in these two criteria have limited the application of those new materials.

## 2. Poly(styrene-4-vinylpyridine) Isoporous Membranes

### a) General of Poly(styrene-4-vinylpyridine) Isoporous Membranes

Block copolymer is a new category of important membrane materials. As a

typical diblock copolymer, poly(styrene-4-vinylpyridine) (PS-P4VP) has a special block structure which includes the hydrophilic “tails” poly-4-vinylpyridine (P4VP) and hydrophobic “heads” polystyrene (PS). The structure of PS-P4VP is depicted in Fig 1.2.1[13].

In 2007 Peinemann proposed a method to integrate copolymer self-assembly and phase inversion[14]. In this method PS-P4VP is cast into an isoporous structure with well-ordered surface, which is suitable for water filtration and gas permeation. In 2010 Nunes *et al.* updated this method using ion complex copper(II) ion-polystyrene-b-poly(4-vinylpyridine) to cast nanoporous films, and the water flux of the new membrane was at least one magnitude order higher than commercially available membranes with comparable pore size[15].

There are many groups focusing their research on PS-P4VP polymeric membranes[16]. Improvements in some parts are under investigation, including materials, solvents, and post-processing techniques. Park *et al.* studied the techniques preparing highly-ordered nanoporous template for PS-P4VP films[17] and the nanofluidics of PS-P4VP copolymer in phase separation[18]. Sohn *et al.* and Yun *et.al.* studied PS-P4VP nanostructures with different nanoparticles[19-21].

In this research the method which Peinemann *et.al.* used in 2007 was followed and improved with the diblock copolymer material poly(styrene-4-vinylpyridine) (PS-P4VP) and the mixed solvent of 1:1:1 (wt%) 1,4-dioxane, N,N-dimethyl formamide and tetrahydrofuran (DOX-DMF-THF, DDT). A general membrane

preparing process included in succession the casting of the PS-P4VP solution onto a given substrate, the evaporation of the solvent for about 20 sec and the immersion of the film into a non-solvent. In this process the PS-P4VP copolymer finished self-assembly and phase inversion, and formed an isoporous structure with a well-ordered surface[14]. The isoporous structure was suited to aqueous filtration and gas permeation, and the permeability of the membranes was evaluated by flux tests.

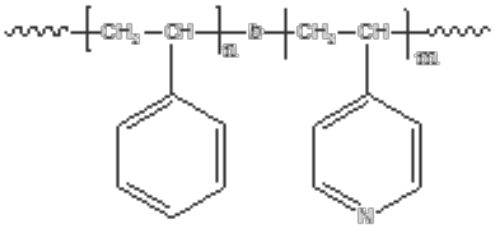

Fig 1.2.1 Structure of PS-P4VP[13]

**b) Water/Gas Flux, Hysteresis and pH-correlation Curves**

Water/gas flux is a crucial variable determined by the pore size for the filtration membranes. A pH-correlation curve (water flux versus pH value) depicts the trend of water flux with increasing or decreasing pH values. A pair of pH-correlation curves includes one pH-increasing curve and one pH-decreasing curve.

Hysteresis is an effect in which the water flux value on the pH-increasing curve is different from that on the pH-decreasing curve at the same pH value, due to joint actions involving the protonation, the stretching of micelle segments and the change of pore sizes. Hysteresis is an important phenomenon observed in block copolymer membranes during aqueous filtration. With $[H^+]$ in the filtered solution increasing

(pH value decreasing) the pore size of the membrane is reduced. The possible mechanism is that $H^+$'s are attached to the nitrogen-ends in a P4VP tails and bring in a positive charge for each tail, and then the positively charged tails are torn apart from each other to stretch the corona segments. This process shrinks the pores while increasing the distance between micelle cores. In general, the force closing the pores is much stronger than that increasing the distance, so the water flux drops dramatically in a low-pH environment. But the distance changing force cannot be neglected when comparing a pair of pH-correlation curves (pH-increasing and pH-decreasing). Because the two forces affect the water flux in different ways, the two curves do not overlap with each other.

Conclusively the main reason for the decreased water flux at a low pH is that the repulsion between protonated P4VP tails increases the micelle distance and shuts down the pores. And the hysteresis comes from the competition of two factors. In order to reduce this and then hysteresis, three ideas were applied in this research: 1) to reduce the protonation, 2) to enlarge the pores, 3) to fix the micelles spatially. And three additives – 1,4-diiodobutane (Sec I.2.c), homo-poly(4-vinylpyridine) (homo-P4VP, Sec I.2.d) and single-wall carbon nanotube (SWCNT, Sec I.2.e) – were introduced respectively based on this analysis.

In this research the pH-correlation curves were created to evaluate the water flux, the extent of hysteresis and the improvement by additives.

### c) Cross-linking and 1,4-diiodobutane

If the nitrogen-ends in P4VP tails are preoccupied – linked to something else in other words – the probability of protonation is reduced. Based on the current knowledge the P4VP block can be cross-linked using dihalobutane through a quatenization reaction. (The mechanism of 4-vinylpyridine groups being cross-linked by dihalobutane is depicted in Fig 1.2.2[22].) This explains why 1,4-diiodobutane ($C_4H_8I_2$, Fig 1.2.3) was used as the cross-linking agent in this research[23,24]. The cross-linking is also able to "fix" the micelle structure and to counteract the distance increase, which reduces the pore shut-down further.

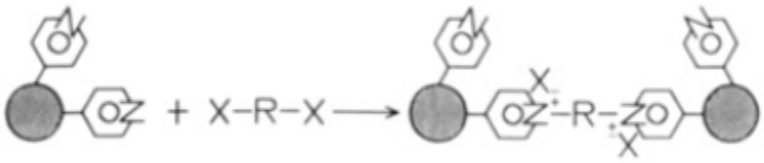


Fig 1.2.2 Reaction Schemes for the Cross-linking Reaction between P4VP Block and Dihalobutane[22]

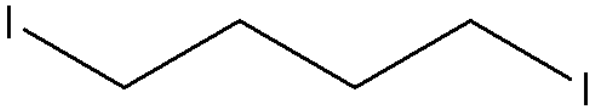

Fig 1.2.3 Structure of 1,4-diiodobutane

**d) Additive Homo-poly(4-vinylpyridine)**

The PS-P4VP micelle structure, which forms the well-ordered surface, is assembled by hydrophobic PS heads and hydrophilic P4VP tails[30]. Homo-poly(4-vinylpyridine) (homo-P4VP, Fig 1.2.4[25]) shares the same P4VP block as the outer micelle. The strong incompatibility between the PS head and the P4VP tail pushes the two parts away from each other. In other words, the homo-P4VP block will insert itself into the pore wall and will result in a greater pore size than a

simple PS-P4VP membrane[26,27]. In this research a small amount of homo-P4VP was added attemptively, and the rebuilt surface and water flux of the (PS-P4VP)-(homo-P4VP) membranes were compared with original ones in order to observe if the previous guess can be confirmed.

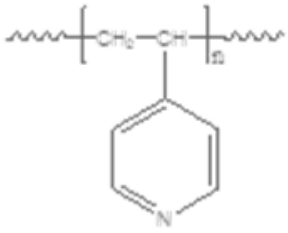

Fig 1.2.4 Structure of Homo-P4VP[25]

**e) Single-Wall Carbon Nanotube**

In order to spatially fix the PS-P4VP micelles and to relieve the distance increase and the hysteresis, a rigid additive to which the micelles can attach is required. Under the circumstances single-wall carbon nanotube (SWCNT) was introduced in this research.

SWCNT has attracted attentions for a variety of potential applications in recent years[28,29]. For example, it is treated as a useful tool for increasing the stability and mechanical property of a polymer material. But the idea with SWCNT added in block copolymer membranes has not yet been widely used in the world. In this research SWCNT was purchased from Sigma-Aldrich (cat. no. 704121), length: 300-2300 nm, diameter: 0.7-1.1 nm).

As is depicted in Fig 1.2.5 and Fig 1.2.6, SWCNT has a graphite-like structure. The nanotubes, to which P4VP hydrophilic tails can attach, are evenly dispersed

within the membranes. And one SWCNT is able to link a series of PS-P4VP micelles together and to partially fix the distance between them. This process supports the isoporous structure and increases the stability of membranes as well.

After SWCNT is introduced to PS-P4VP membranes, the distance between two micelles is only slightly changed by protonation as a series of micelle cores are linked to SWCNT. In this case only the pore-closing force takes effect and the two pH-correlation curves overlap with each other. This process reduces the hysteresis and thus can be proved if the hysteresis is relieved[30].

PS-P4VP-SWCNT membranes can also be prepared DOX-DMF-THF mixing solvent. However, because SWCNT will not be well-dispersed a little in DOX after about two weeks, the polymer solution can be prepared in a different way using copper acetate ($Cu(Ac)_2$) as a substitute of DOX (discussed in Sec II.2.a).

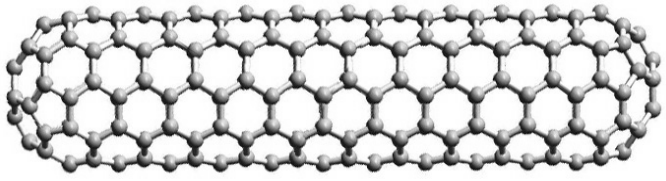

Fig 1.2.5 Graphite-like Structure of SWCNT[31]

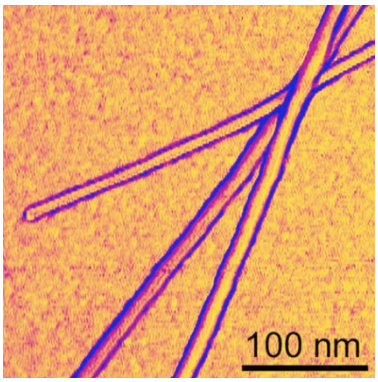


Fig 1.2.6 Microscopic Image of SWCNT[32]

### f) Solvent

In this research, two solvents were used in preparing the primary copolymer solutions – the mixture DDT containing 1:1:1 (wt%) dioxane (DOX), N, N-dimethyl

formamide (DMF), and tetrahydrofuran (THF), used for most samples; and CDT containing copper acetate ($Cu(Ac)_2$), DMF, and THF (recipe in Table 2.3.5), used for some PS-P4VP-SWCNT samples. The reason why DDT ternary solvent is discussed here as it was applied most.

Nunes *et al.* discussed different combinations of DOX, DMF and THF, and proved that only DDT led to PS-P4VP membranes with desired ordered pored surface, while the DMF-THF solvent produced a cylindrical structure and DMF-DOX or THF-DOX created the "disordered" pored morphology[30]. Also in their research a correlation was revealed between the copolymer self-assembly in the primary solution and the membrane morphology. Primary solutions prepared with DDT had the maximum micelle order and built most ordered membranes in the end[30].

Based on Israelachvili's theory, the self-assembly structure is determined by two factors – a balance between solvent-phobic and solvent-philic interactions, and the relative block sizes[34]. Thermodynamically the micelles tend to form with solvent-philic P4VP tails outside to protect the solvent-phobic PS heads, and a certain level of "molecular frustration" is also necessary for the characteristic micelle curvature. A three-dimensional "frustration" leads to spherical micelles as expected, while if "frustration" is restricted to two dimensions, a cylindrical structure is formed[30].

A delicate self-consistent field (SCF) model can be created to describe the micelle formation theoretically, but a rough quantitative consideration is to

correlate the morphology to a molecular packing parameter p which can be calculated as follows (Eqn 1.2.1)[30,35].

$$p = \frac{V_0}{a_0 d} \quad \text{(Eqn 1.2.1)}$$

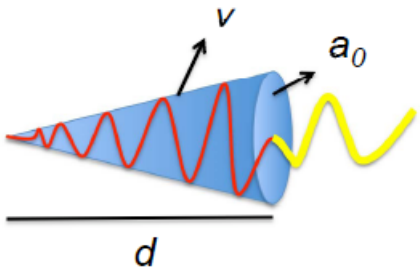


Fig 1.2.7 Pictorial Diagram of Three Variables Determining Molecular Packing Parameter

, in which V is the volume of one single PS block and d is its length, and $a_0$ is its optimal surface area at the block interface (Fig 1.2.7). Spherical micelles are formed when $p \leq 1/3$; cylindrical micelles are formed at $1/3 < p \leq 1/2$; and layers are formed when $1/2 < p \leq 1$. If the attraction between chains predominates, $a_0$ will decrease and p will increase, and cylindrical micelles or even layer structure will be favored; and if repulsion predominates, $a_0$ will increase and p will decrease, and spherical micelles will be favored[30].

In different combinations of solvents, the repulsion and attraction weigh differently and will result in different $a_0$ and p values. Concerning the polarity, DOX<THF<DMF[30], so DOX tends to interact with PS heads and increase $a_0$, while DMF tends to interact with P4VP tails and decrease $a_0$. The effect of THF lies between DOX and DMF. If $Cu(Ac)_2$ is not considered, the 1:1:1 DDT solvent gives the

satisfactory result[30].

Further, however, the solvent is not the only factor that determines the membrane morphology. All of the three variables, V, d and $a_0$ are influenced by the block size of the PS-P4VP copolymer as well, so polymer screening is necessary to pick up the copolymer best suited to DDT comparing their micelle shapes.

**g) Surface Topography and Atomic Force Microscopy**

All through this research, the surface topography of all membrane samples were scanned and observed using atomic force microscopy (AFM). AFM is a very high-resolution (<1nm) scanning probe microscopy, which consists of a cantilever with a sharp tip (probe) at its end (Fig 1.2.8)[36]. When the tip is brought to the proximity of the sample surface, a force will occur between the tip and the surface (van der Waals forces, chemical bonds, electrostatic forces, magnetic forces, etc.) and will cause the deflection of the cantilever according to Hooke's law[37]. This deflection can be measured using a laser (Fig 1.2.9). A comprehensive image can be obtained while the cantilever scans the whole surface and collects all deflections[37].

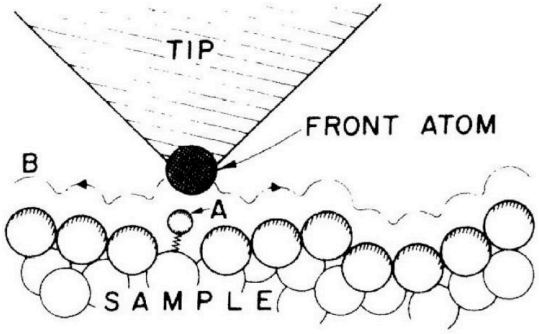


Fig 1.2.8 Operation Description of AFM

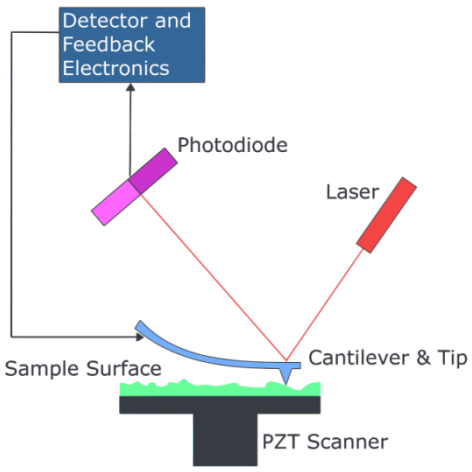


Fig 1.2.9 Block Diagram of AFM

The AFM machine (Veeco Dimension Icon Atomic Force Microscope) has three operation modes: height sensor, phase and altitude error. In the "Experiment and Calculations" part of this thesis, the AFM images in the high sensor mode and the phase mode are attached, as those three modes represent similar surface topography.

## 3. Objective of This Thesis Research

In the field of aqueous separation, membrane process is more efficient and more economic than routine ways. And carbon dioxide separation with membranes has become a hot spot in gas separation. These technologies can help to save the resources and energy, especially in drought or resource-poor areas[2].

Membrane research turned out very interesting to me and therefore I joined in Advanced Membrane and Porous Materials Center at KAUST. My first research experience related to isoporous membranes was in 2010 summer when I was working in the Wiesner group at Cornell University, and it gave me a deeper understanding of this field.

My master's thesis research focused on PS-P4VP isoporous membranes in the Peinemann group. As stated in Sec I.2, PS-P4VP is a suitable material for isoporous membranes. It was shown that the membranes made of PS-P4VP, especially its copper (II) complex, had very good water flux[14,15]. The objective of this research was to further explore and improve Dr Peinemann's new method, including the search of a reliable membrane preparation procedure, the investigation of membrane properties, and the introduction of additives and post-processing techniques that might improve the properties. The key additive in this research was single-wall carbon nanotube (SWCNT).

## 4. Structure of This Thesis Research

This PS-P4VP isoporous membrane project was comprised of the following parts.

First of all, polymer screening was performed among four PS-P4VP copolymers (obtained from Polymer Source™, Inc., Canada) to pick up the best membrane material.

Secondly, membranes were cast from PS-P4VP solutions. Surface topography of the membranes was characterized by atomic force microscopy (AFM) and the pH-correlation curves were created by water flux tests under a series of gradient pH buffers.

Based on the previous analysis, additives (1,4-diiodobutane, SWCNT, homo-P4VP and $Cu(Ac)_2$) were added respectively to observe the change of

membranes properties if any. Their surface topography and pH-correlation curves were compared with the original membranes.

# Chapter II

# EXPERINENTS and CALCULATIONS

## 1. Polymer Screening

The four candidate samples for screening were P8207-S4VP, P3806-S2VP, P3910A-S4VP* and P5722-S4VP (Polymer Source™, Inc., Canada). Each sample has a its own $M_n$ and $M_w/M_n$ ratio, both of which are significant parameters that determine the spatial structure of the membranes. Their physical properties are listed in Table 2.1.1.

Table 2.1.1 Physical Property of Polymer Candidates

| Sample No. | Catalog No. | $M_n$ ($10^3$ g/mol) | $M_w/M_n$ |
|---|---|---|---|
| P8207 | P8207-S4VP | 130-b-75.0 | 1.25 |
| P3806 | P3806-S2VP | 101-b-29.0 | 1.60 |
| P3910 | P3910A-S4VP* | 109-b-30.0 | 1.15 |
| P5722 | P5722-S4VP | 138-b-41.0 | 1.15 |

All samples were tested in the 1:1:1 DOX-DMF-THF (DDT) solvent following the procedures in Sec II.2. According to the comparison of the AFM (Veeco Dimension Icon Atomic Force Microscope) images and the membrane properties (Table 2.1.1), finally P3910 and P5722 were chosen because of the well-ordered isoporous strutures of their membranes.

## 2. Membrane Synthesis

Following is the general procedure of membrane preparation in this research.

### a) Preparation of Polymer Solution

The solution preparation step was slightly different when different additives were used.

If the membranes contained PS-P4VP only, the copolymer (160 mg of P5722 or 200 mg of P3910) were dissolved in the solvent (800 mg of 1:1:1 DDT or $Cu(Ac)_2$-DMF-THF, CDT) and stirred for a few hours until the transparent primary solution was formed. The concentration (wt%) of the primary solution was 16.6% for P5722 or 20.0% for P3910. If there were bubbles produced in the solution, the solution was left still until all bubbles were gone.

If homo-P4VP was used, it was dissolved into the prepared primary solution. The new solution was stirred for several hours until it turned clear again.

If SWCNT was used, the primary solution should be prepared in a different way. SWCNT was most soluble in DMF, so at first SWCNT was dispersed in the pure DMF for 10 min by ultrasonic using a Sonics VCX 130. DOX and THF were then added to this SWCNT-DMF mixture following the same weight fraction (1:1:1 for DDT). PS-P4VP was later dissolved in this well-dispersed SWCNT-solvent mixture and stirred for a few hours to form the primary solution. The solution was black and not transparent but homogenous.

In general the SWCNT-DDT mixture was homogenous within a short duration but in two weeks a slight phase separation would be observed. $Cu(Ac)_2$ (copper acetate)-DMF-THF (CDT) mixed solvent can also induce the self-assembly and phase inversion of PS-P4VP[15], so $Cu(Ac)_2$ was attempted to replace DOX to make polymer

solution and then cast into films. These membranes prepared in CDT were also checked under AFM to observe any possible improvement.

**b) Film Casting**

The solution was cast on the substrate using a proper casting blade. Two types of substrates were used in this research: 1) Clean glass slides, upon which the solution was cast straightly using a casting blade (Fig 2.2.1, thickness was adjusted to 200 μm). 2) Non-woven polyethylene terpthalate (PET, Fig 2.2.2) substrate membranes, which were stuck to the glass slides using water-soluble glue and scotch tapes to keep out the air. (The residual air under the substrate could make the membrane uneven.) The casting blade was adjusted to 250 μm. The volume of polymer solution used for casting was dependent to the size of the film, and a good range was 300 μL ~ 800 μL.

Fig 2.2.1 Film Casting Blade

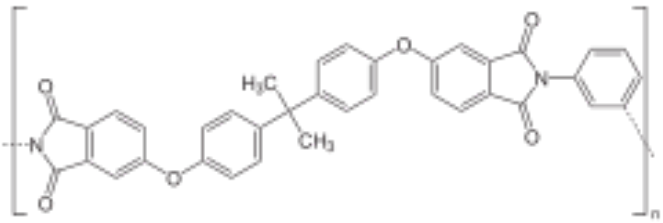


Fig 2.2.2 Structure of Polyethylene Terpthalate (PET)

After the casting the primary film was exposed at room temperature for 15~20 sec for the solvent to evaporate.

**c) Film Solidification**

After the 15~20 sec evaporation, the primary film was immediately bathed into de-ionized water and stayed for more than 30 min in order to solidify the inner structure and to finish the phase inversion process. Then the film was washed with a small amount of ethanol and dried in the fume hood.

The dried film was cut into circular membranes with a fixed diameter using scissor and hammer. The membranes were labeled and archived for flux tests, pH correlation curves or post-processing.

**d) Post-Processing**

If the cross-linking inducer 1,4-diiodobutane was used, the membranes were bathed in the diluted 1,4-diiodobutane-ethanol solution at 60□ for at least 4 h or overnight. The post-processed membranes were ready for AFM imaging and water/gas flux tests.

## 3. Supplemental Reagents

**a) 1,4-diiodobutane**

1,4-diiodobutane (purchased from Sigma-Aldrich) is a good cross-linking agent and its physical constants are shown in Table 2.3.1. Based on the previous research experiences, the concentration of 1,4-diiodobutane in the solution should be around 1%~2%. Three groups treated in three different cross-linking environments were

compared in this research (Table 2.3.2).

Table 2.3.1 Physical Constants of 1,4-diiodobutane

| Mol. Form. | Mol. Wt. | mp (°C) | Other bp (°C) | ρ(g/cm$^3$) | Solubility |
|---|---|---|---|---|---|
| $C_4H_8I_2$ | 309.916 | 5.8 | 125[15] dec | 2.349425 | i H2O; sl ctc; s os |

Table 2.3.2 Three Cross-linking Environments

| Group No. | Chemical Environment | Reaction Duration |
|---|---|---|
| 1 | 1% 1,4-diiodobutane in ethanol | 4h |
| 2 | 2% 1,4-diiodobutane in ethanol | 4h |
| 3 | de-ionized water | 4h |

**b) Single-Wall Carbon Nanotube**

SWCNT (*Sigma-Aldrich* (cat. no. 704121), length: 300-2300 nm, diameter: 0.7-1.1 nm) was introduced to enhance the rigidity of the membranes and to reduce the hysteresis. The mass of SWCNT and PS-P4VP used in this research were calculated as follows.

Assuming that in the primary solution contains a mg of PS-P4VP, b mg of SWCNT and 3c g of 1:1:1 DDT solvent.

To make sure of the best structures, the concentration (wt%) of PS-P4VP in the primary solution is fixed to a optimal value (16.6% for P5722 and 20.0% for P3910):

$$C_{\text{PS-P4VP}} = \frac{0.001a}{0.001(a+b)+3c} \cong \frac{a}{a+3000c}\left(a >> b\right) \quad \text{(Eqn 2.3.1)}$$

And the concentration of SWCNT in the same solution ($C_1$) is

$$C_1 = \frac{0.001b}{0.001(a+b)+3c} \cong \frac{b}{a+3000c} = \frac{bC_{\text{PS-P4VP}}}{a} \quad \text{(Eqn 2.3.2)}$$

Since some of solvent was evaporated during the solidification, it is improper to use the mass of solvent in the concentration. Instead, the mass ratio of SWCNT to polymer ($C_2$) is used

$$C_2 = \frac{b}{a} \quad \text{(Eqn 2.3.3)}$$

$$C_1 = C_2 C_{\text{PS-P4VP}} \quad \text{(Eqn 2.3.4)}$$

In order to investigate how the inner and surface structure of the membranes were affected by the SWCNT concentration, groups with different SWCNT concentrations were prepared and compared (Table 2.3.3).

Table 2.3.3 Different Concentrations of SWCNT in Solutions and Membranes

| Mass (SWCNT) (mg) | Mass (DMF) (g) | P5722 | | | P3910 | | |
|---|---|---|---|---|---|---|---|
| | | Mass (P5722) (mg) | $C_1$ (%) | $C_2$ (%) | Mass (P3910) (mg) | $C_1$ (%) | $C_2$ (%) |
| 3 | 5 | 160 | 0.017 | 0.10 | 200 | 0.016 | 0.08 |
| 6 | 5 | 160 | 0.033 | 0.20 | 200 | 0.032 | 0.16 |
| 12 | 5 | 160 | 0.066 | 0.40 | 200 | 0.064 | 0.32 |

**c) Homo-poly(4-vinylpyridine)**

Homo-P4VP was able to insert itself into the PS-P4VP micelles and to affect the inner and surface structure. The physical properties of homo-P4VP are listed in Table 2.3.4.

Table 2.3.4 Physical Property of Homo-P4VP

| Catalog number | $M_w$ ($10^3$g/mol) | $M_w/M_n$ |
|---|---|---|
| P130-4VP | 36.3 | 1.17 |

**d) Copper Acetate**

As discussed in Sec II.2.a, SWCNT-DDT mixture is not stable as SWCNT is not

very soluble in DOX, therefore $Cu(Ac)_2$ was introduced as a substitute of DOX. The new mixing solvent is called CDT ($Cu(Ac)_2$-DMF-THF) for short. A $Cu^{2+}$ can bond to the nirogen-end in a P4VP tail, which indicates that $Cu(Ac)_2$ solvent mixture have the ability to induce copolymer's self-assembly and phase inversion[33]. Two mixing solvents were used to make the polymer solution (Table 2.3.5) and compared in this research.

Table 2.3.5 Recipe of Solutions using $Cu(Ac)_2$

| | |
|---|---|
| Solvent I | 7g DMF + 3g THF + 150 mg $Cu(Ac)_2$ |
| Solvent II | 7g DMF + 3g THF |
| Polymer Solution 1 | 100 mg Solvent I + 200 mg P5722 |
| Polymer Solution 2 | 700 mg Solvent II |

## 4. Surface Topography

The surface topography was observed by optical microscopy and AFM (Veeco Dimension Icon Atomic Force Microscope) following the procedure below, and results are listed in Sec III "Results and Discussions".

1) The machine was opened and membrane sampes were setup into the chamber.

2) The focus was adjusted until a microscopic surface topography was presented on the screen. The photos were saved to help identify the general surface structure.

3) The AFM scanning was operated and recorded.

## 5. Flux/Permeance Test and pH-Correlation Curves

### a) Calculation of the Water and Gas Flux/Permeance

Since PS-P4VP membrane is a good material for aqueous seperation, its water and gas flux are the most important parameters to be tested. Water permeability (P) and permeance (J) of membranes can be calculated as follows.

$$P = \frac{Vl}{At\Delta p} \quad \text{(Eqn 2.5.1)}$$

$$J = \frac{P}{l} = \frac{V}{At\Delta p} \quad \text{(Eqn 2.5.2)}$$

V is the volume of the solution, l is the thickness of the membrane, t is the time for solution to pass through the membrane, and Δp is the pressure difference between feed and permeate, which can be measured using a barometer. J, also called "flux" all through this research, is the permeance of the membrane and the most important parameter under investigation.

The same equation is used in gas flux calculation, but V is the volume which the soap bubble passes during time t.

**b) Procedure of Water Flux/Permeance Test**

1) A membrane slide was fixed into the cell of water permeability instrument (Amicon dead-end filtration cell, 10 mL, Pmax 75 psi, 5.3 kg/cm$^2$) and moistened with the same solution for a few times.

2) The instrument was filled with solution (de-ionized water, or acidic/basic solution) and then sealed. The instrument was placed on the turntable with the speed 100 round per min, in order to make sure the solution is isotropic. One end of the instrument was connected to the nitrogen gas, and the other to a measuring

cylinder.

3) After the opening of the nitrogen valve, the first 1~2 mL of solution was discarded. When the fluid turned smooth and stable, the measuring cylinder was used to hold the solution poured out from the instrument.

4) When the solution was being poured, the time, the nitrogen pressure and the solution volume were recorded and the flux was calculated.

**c) Procedure of Gas Flux/Permeance Test**

1) A membrane slide was fixed into the stainless millipore cell of gas permeability instrument (Millipore Co., 150/275 Psi MAX) and was kept dry.

2) The instrument was sealed, connected to the soap bubble flow meter and the nitrogen gas at the other end.

3) After the opening of the nitrogen valve, the first several mililiter of gas was discarded until the force pressure became a constant.

4) When the bubble started to move upwards, the time, the nitrogen pressure and the volume that bubble passed were recorded, and the flux was calculated.

**d) Creation of pH-Correlation Curves**

The procedure of pH-correlation experiment based on water flux test was shown below. A series of buffer solutions were prepared with gradient pH values. In this research the pH of the buffers used were 1.9, 3.1, 4.2, 4.9, 6.4, 7.1, 8.0, 9.0, 9.6, 10.0 and 11.2.

1) A membrane slide was installed into the water permeability instrument and

rinsed with the pH=1.9 buffer for at least 20mins.

2) The rinsing solution was discarded and the flux was tested using a new pH=1.9 buffer.

3) The device and the membrane slide were rinsed with the pH=3.1 buffer for more than 5 min, and then the flux was tested using a new pH=3.1 buffer.

4) Step 3) was repeated using buffers with other pH values in an increasing order. In this way the pH-increasing curve was created.

5) The pH-decreasing curve was created by repeating (3)~(4) (starting from the pH=11.2 buffer) in a decreasing order.

# Chapter III

# RESULTS and DISCUSSIONS

## 1. Appearances of Films and Membranes

### a) Color

The original PS-P4VP membranes with no additives are all white.

The membranes post-processed with diluted 1,4-diiodobutane solution are yellow, and the ones treated with 2% solution are darker than the ones with 1% solution.

The PS-P4VP-SWCNT membranes are all grey. The higher the SWCNT concentration is, the darker the membrane is.

Therefore, the colors of the membranes are affected by the additives.

### b) Optical Microscopy Images

All the optical microscopy images of membranes are listed in Fig 3.1.1~3.1.8.

The original PS-P4VP membranes (both P5722 and P3910, Fig 3.1.1~3.1.4) have smooth, dense and homogenous surfaces. The PS-P4VP-SWCNT membrane (Fig 3.1.5~3.1.6) presents a similar surface while at the spots of the SWCNT the color is darker and the structure is denser.

However, the (PS-P4VP)-(homo-P4VP)-SWCNT membrane presents an uneven surface with holes (Fig 3.1.7~3.1.8), because homo-P4VP has dragged the P4VP tail

out of the surface and has broken the micelle. This phenomenon is more serious in P5722-P1304 membranes as the P5722 molecules are bigger than P3910.

From these images it is clearly that the membranes added with homo-P4VP were not homogeneous, not well-ordered and not even; for all the rest were just homogeneous and even surface, but no further information.

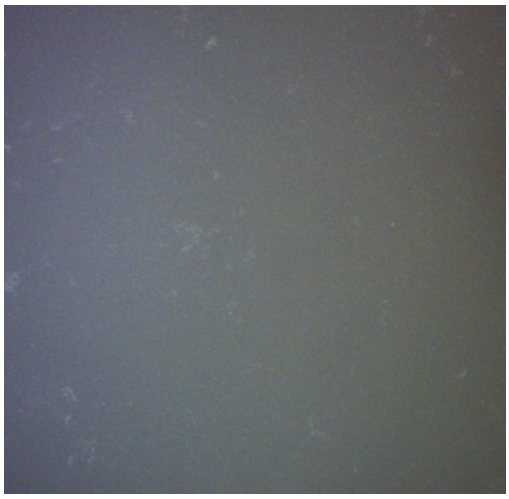

Fig 3.1.1 P5722+DDT

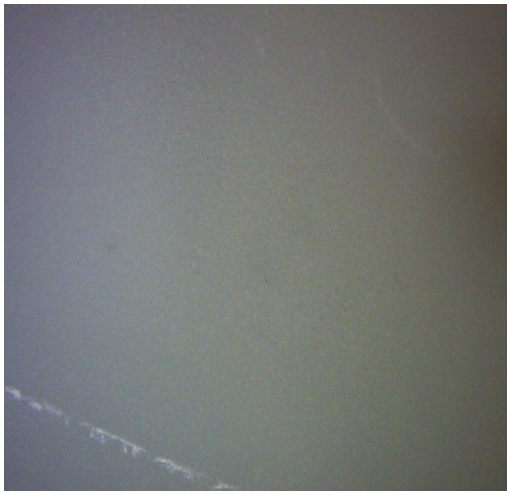

Fig 3.1.2 P3910+DDT

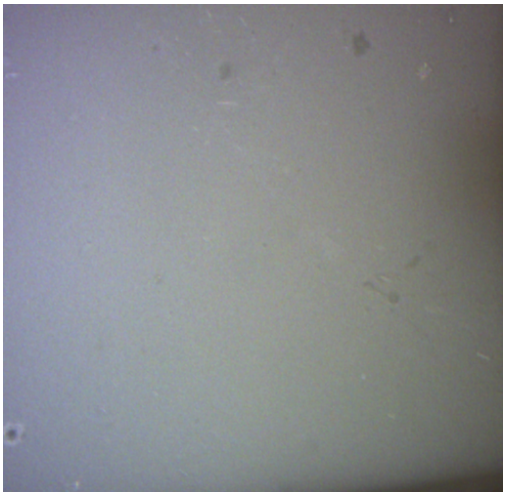

Fig 3.1.3 P5722-SWCNT+DDT

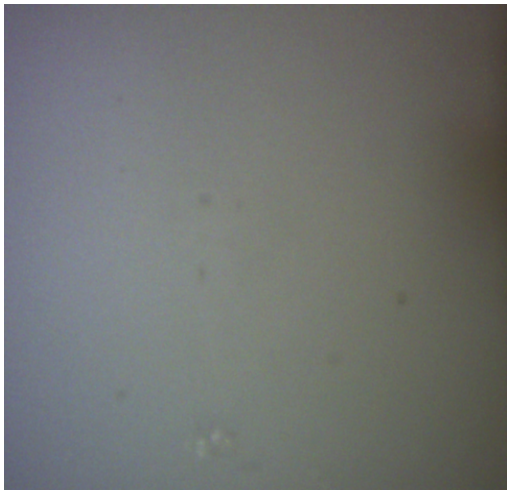

Fig 3.1.4 P3910-SWCNT+DDT

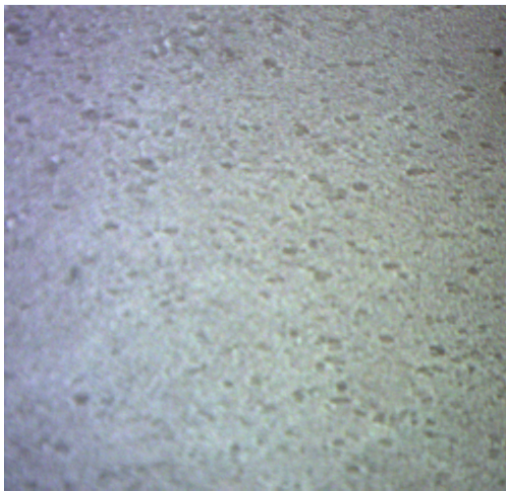

Fig 3.1.5 P5722-P1304-SWCNT+DDT

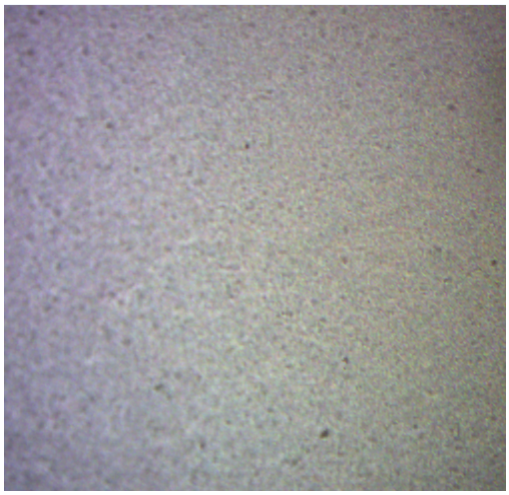

Fig 3.1.6 P3910-P1304-SWCNT+DDT

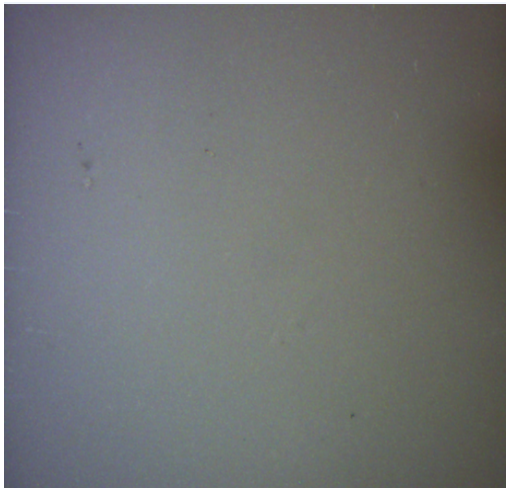

Fig 3.1.7 P5722+CDT

Fig 3.1.8 P3910+CDT

The PS-P4VP membranes prepared in CDT solvent are similar to original PS-P4VP ones on the surface. Therefore the surface structures were not affected by CDT on a general microscopic scale.

**c) Comparison between Two Substrates**

The films cast straightly onto the glass slides are soft and brittle, which makes it impossible to cut into membranes. But there is no problem preparing AFM samples.

The films cast on non-woven PET substrate membranes are flexible and stable, and thus easy to cut into membranes for the future research. All the related researches which require a good membrane strength, like flux tests and pH-correlation curves, were done on the membranes cast on PET substrate membranes.

**d) Effect of Single-Wall Carbon Nanotube**

With the addition of SWCNT, the membranes become more stable, more rigid and more durable than original ones. But there was no proper instrument to test the precise mechanical strength.

## 2. Atomic Force Microscopy Images

**a) Polymer Screening**

The AFM images of the membranes made from the four polymer candidates are all listed in Fig 3.2.1~3.2.8.

1) P8207-S4VP (P8207)

P8207 membrane shows a lamellar surface under AFM (Fig 3.2.1~3.2.2). It is an interesting well-ordered structure but not isoporous, and the surface is not hexagonal either. Therefore P8207 is not a good candidate of water filtration membranes.

2) P3806-S2VP (P3086)

No periodic surface of P3806 is found (Fig 3.2.3~3.2.4), which indicates that it is not a good candidate. And the films are highly fragile.

3) P3910A-S4VP* (P3910)

Well-ordered isoporous hexagonal surface are observed (Fig 3.2.5~3.2.6), and the pore diameter is around 30 nm. The membranes are stable and flexible enough for post-processing. So P3910A-S4VP* is a good candidate for material separation and was chosen in this research.

4) P5722-S4VP (P5722)

The surface structure and the pore size of P5722 (Fig 3.2.7~3.2.8) are very similar to P3910 , and the membranes are even more flexible. So P5722 was also chosen.

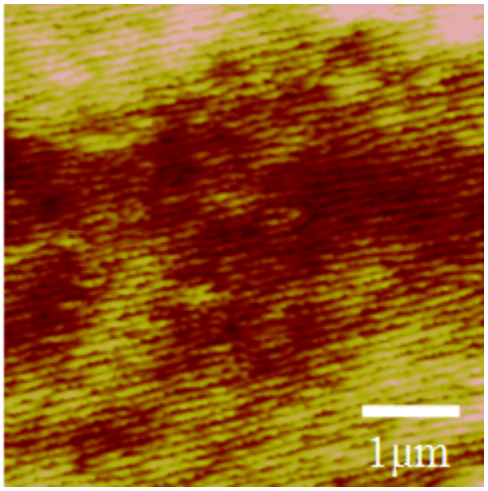


Fig 3.2.1 P8207 (Height Sensor)

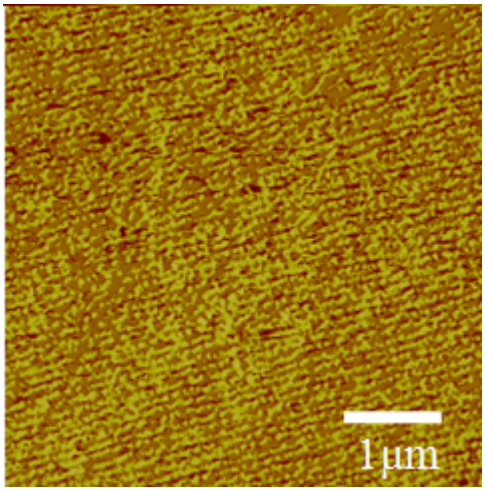


Fig 3.2.2 P8207 (Phase)

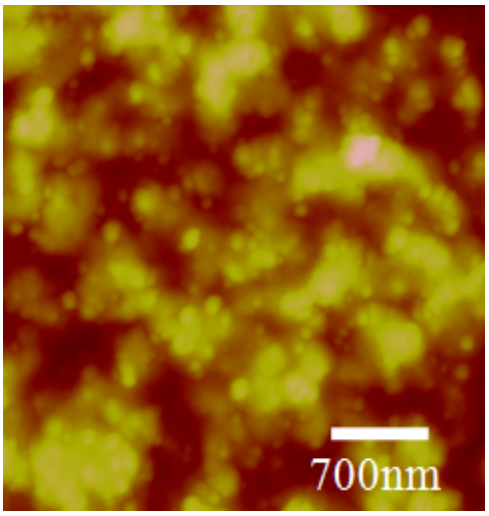


Fig 3.2.3 P3806 (Height Sensor)

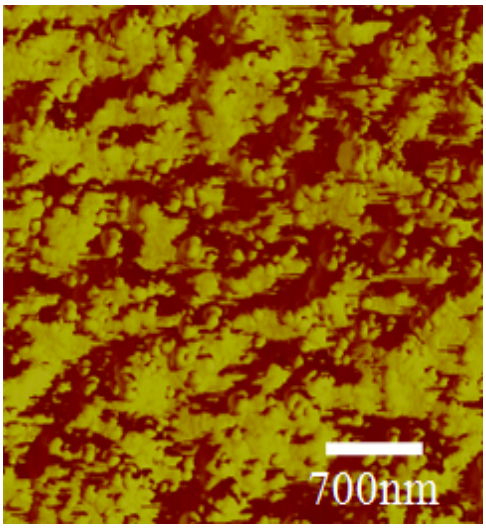


Fig 3.2.4 P3806 (Phase)

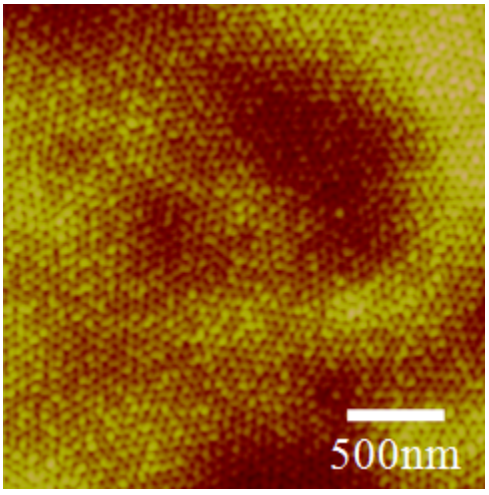


Fig 3.2.5 P3910 (Height Sensor)

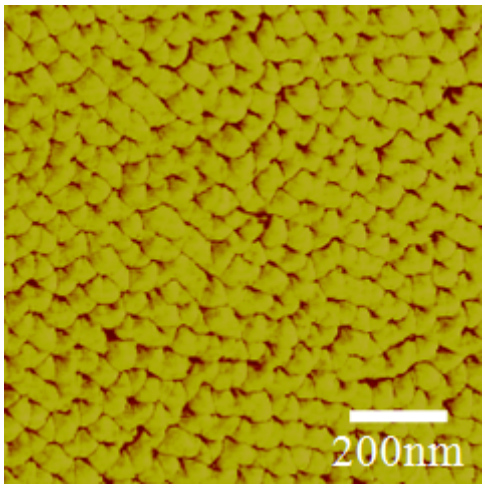


Fig 3.2.6 P3910 (Phase)

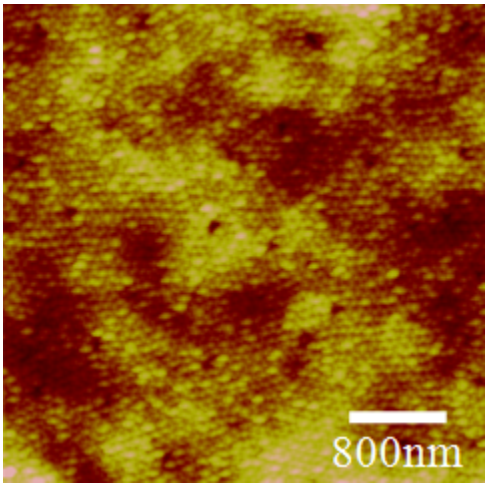


Fig 3.2.7 P5722 (Height Sensor)

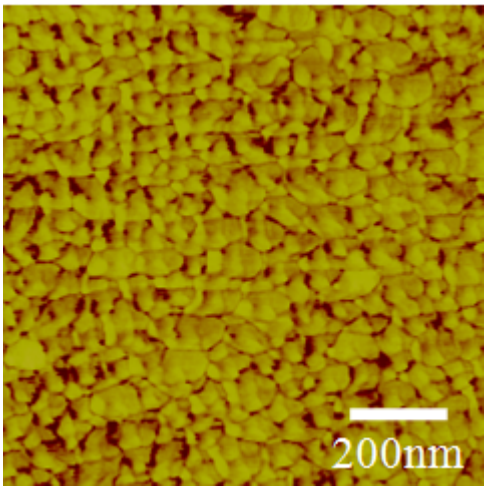


Fig 3.2.8 P5722 (Phase)

**b) PS-P4VP-SWCNT Membranes**

The AFM images of the P5722-SWCNT and P3910-SWCNT are listed in Fig 3.2.9~3.2.12.

1) P5722-SWCNT

P5722-SWCNT membrane presents a well-ordered isoporous hexagonal surface (Fig 3.2.9~3.2.10), which is much better than original P5722. And mechanical strength is also improved to a better post-processing and application.

2) P3910-SWCNT

P3910-SWCNT membrane also presentss a well-ordered isoporous hexagonal surface (Fig 3.2.11~3.2.12) which is better than original P3910. And mechanical strength is improved as well.

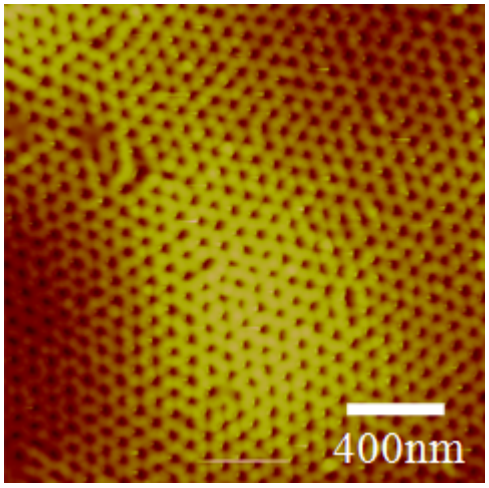


Fig 3.2.9 P5722-SWCNT (Height Sensor)

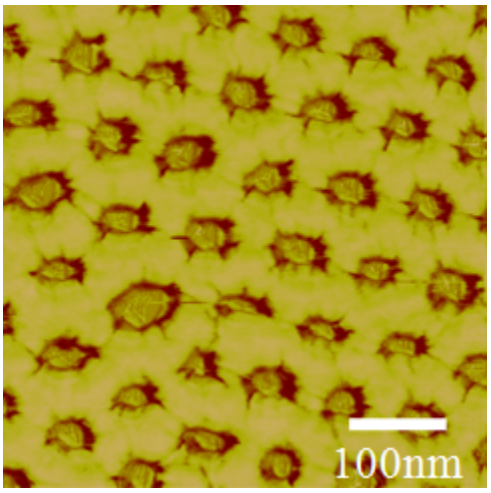


Fig 3.2.10 P5722-SWCNT (Phase)

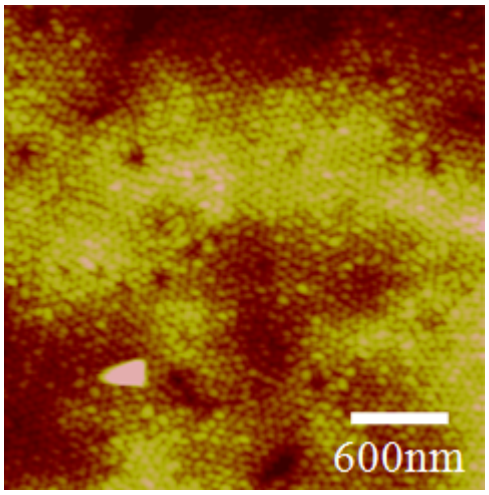


Fig 3.2.11 P5722-SWCNT (Height Sensor)

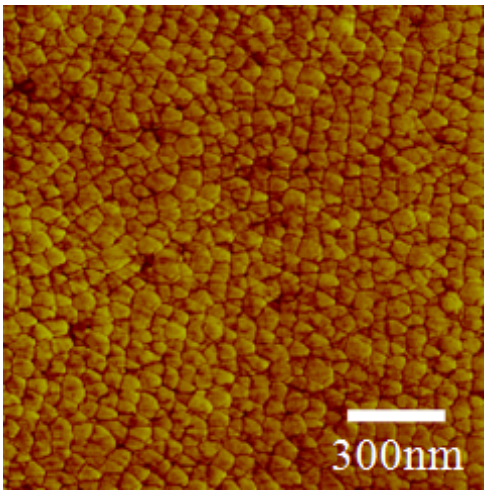


Fig 3.2.12 P3910-SWCNT (Phase)

### c) (PS-P4VP)-(homo-P4VP) Membranes

The AFM images of the P5722-P1304 and P3910-P1304 (with or without addition of SWCNT) are listed in Fig 3.2.13~3.2.20.

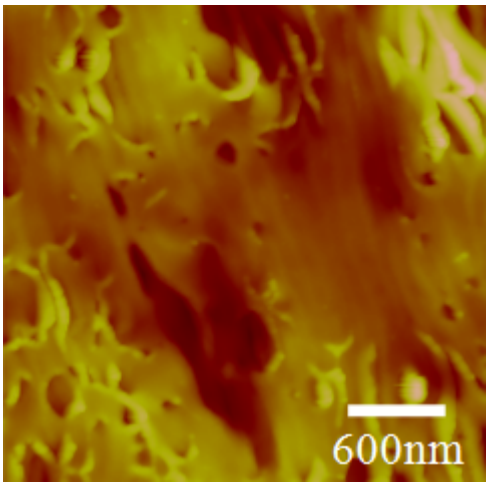


Fig 3.2.13 P5722-P1304 (Height Sensor)

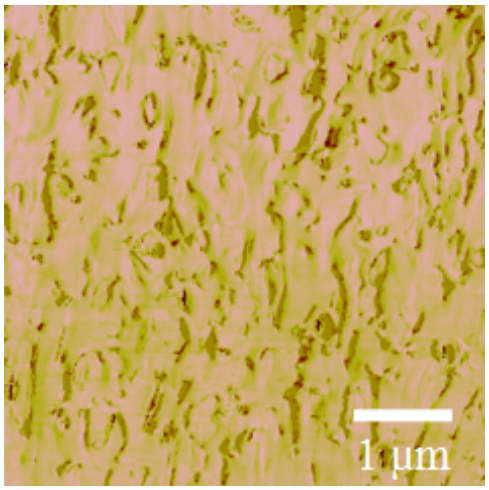


Fig 3.2.14 P5722-P1304 (Phase)

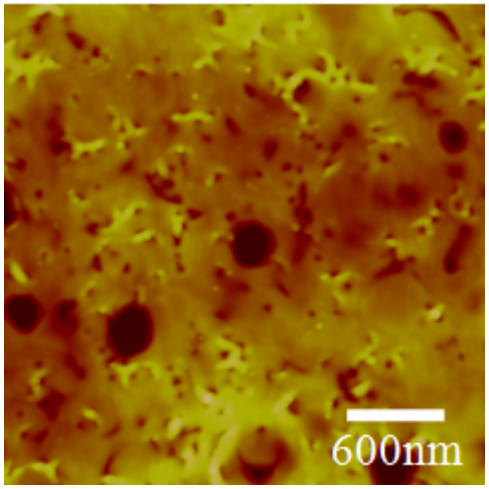


Fig 3.2.15 P3910-P1304 (Height Sensor)

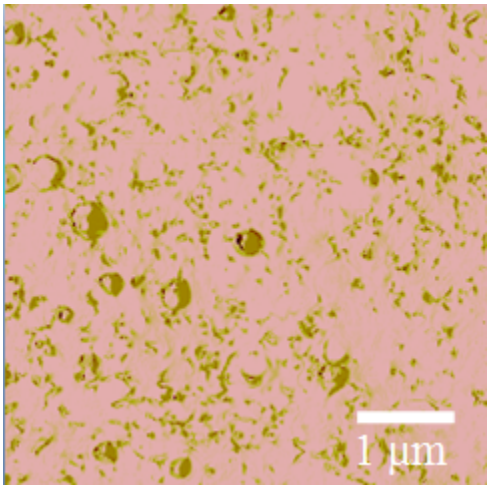


Fig 3.2.16 P3910-P1304 (Phase)

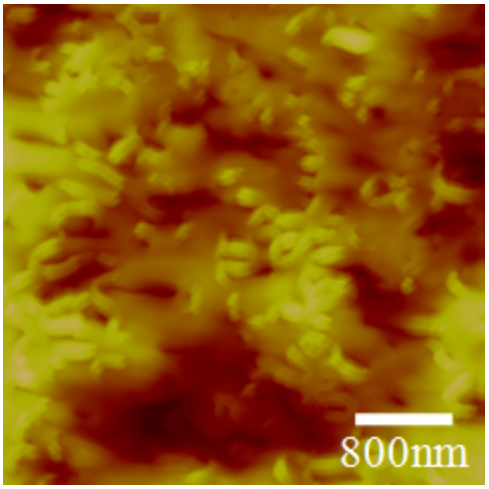


Fig 3.2.17 P5722-P1304-SWCNT (Height sensor)

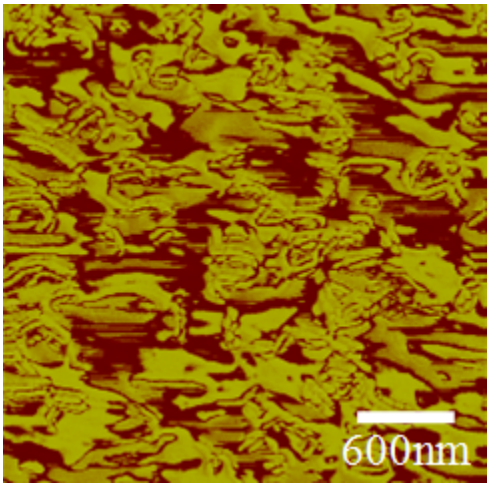


Fig 3.2.18 P5722-P1304-SWCNT (Phase)

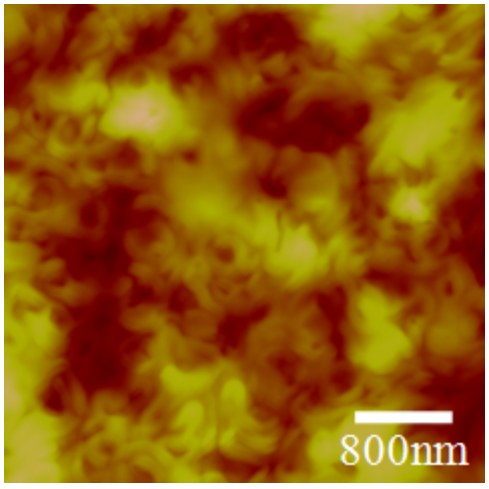


Fig 3.2.19 P3910-P1304-SWCNT (Height Sensor)

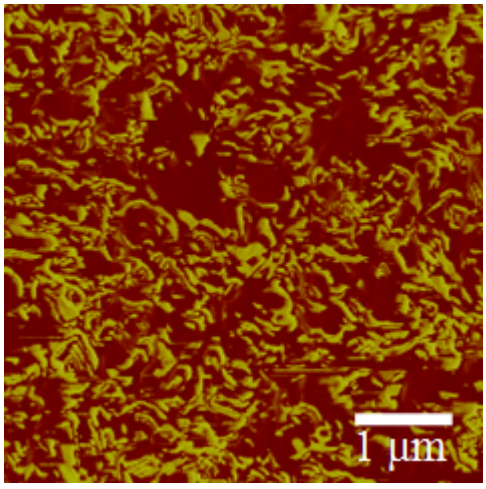


Fig 3.2.20 P3910-P1304-SWCNT (Phase)

A short-range self-assembly structure is found in both membranes without addition of SWCNT (Fig 3.2.13~3.2.16). But they are still not well-ordered in a long range – the structure is not isoporous, and the surface is not hexagonal. Such membranes are not suitable for post-processing and future research. Homo-P4VP has inserted itself into PS-P4VP micelles and has disturbed inner and surface structrue which accounts for the disordered surface structures. Addtion of SWCNT has a small improvement (Fig 3.2.16~3.2.20) which not enough to make suitable membranes.

**d) Membranes Prepared in $Cu(Ac)_2$-DMF-THF Solvent**

Fig 3.2.21~3.2.24 list P5722 and P3910 membranes prepared by the author in the CDT solvent. Both of them present the short-range self-ssembly structure only, though P3910 is better than P5722. They are not suitable for aqueous separations and thus CDT was not used in the following research.

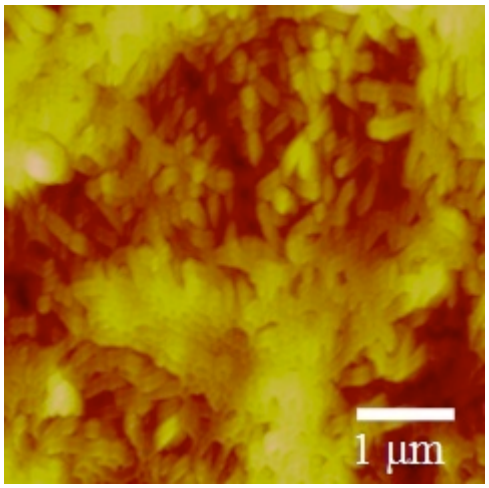


Fig 3.2.21 P5722+CDT (Height Sensor)

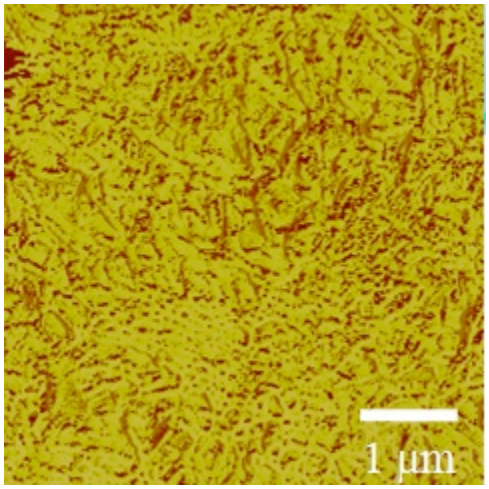


Fig 3.2.22 P5722+CDT (Phase)

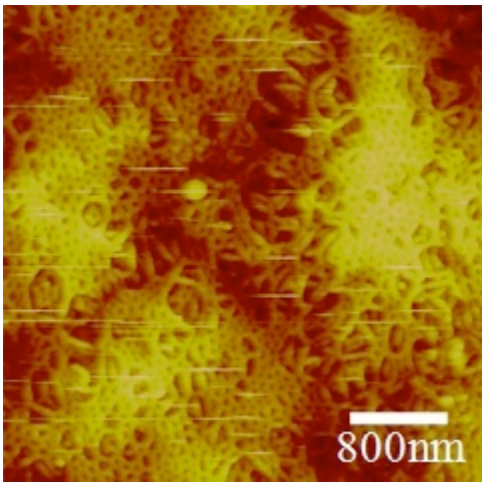


Fig 3.2.23 P3910+CDT (Height Sensor)

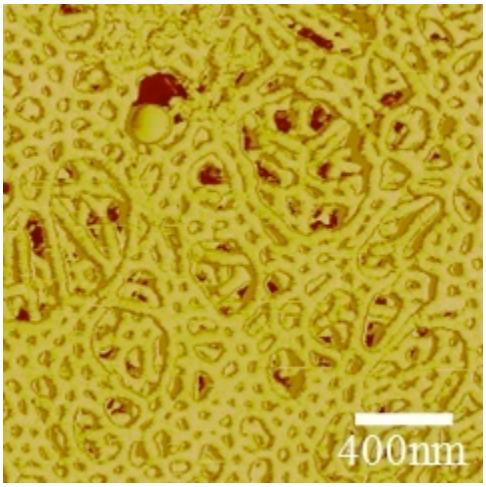


Fig 3.2.24 P3910+CDT (Phase)

And unfortunately, the polymer purchased from Polymer Source™, Inc. run out of stock before any improvement was made in synthesis procedure using CDT. SWCNT-DDT mixture, rather than CDT, was still used but was prepared right before the membrane casting, in order to minimize the effect from phase separation.

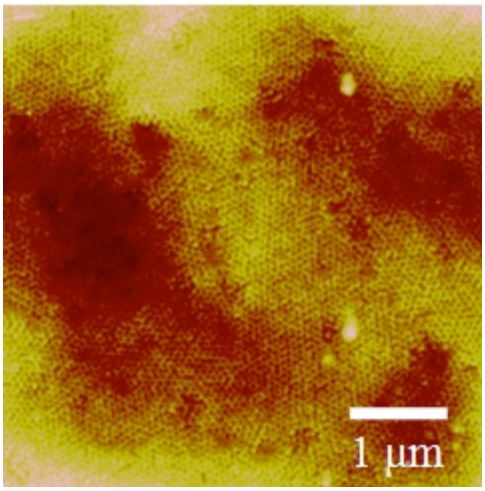


Fig 3.2.25 P5722+CDT by Dr. Peinemann (Height Sensor)

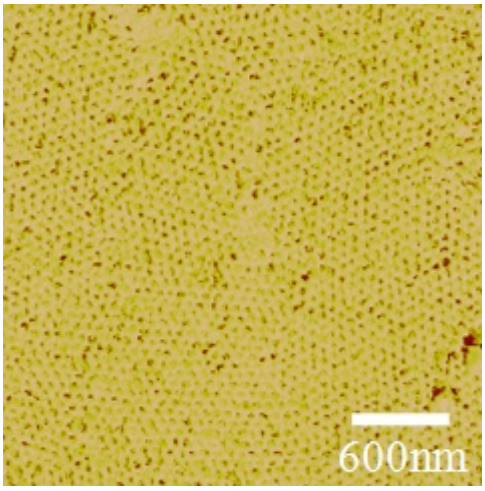


Fig 3.2.26 P5722+CDT by Dr. Peinemann (Phase)

Fig 3.2.25 and 3.2.26 show a better P5722+CDT membrane prepared by the author's advisor, Dr Peinemann. The surface structure was much better-ordered. This proved that CDT was indeed proper solvent mixture for PS-P4VP membrane

upon good casting skills.

## 3. Water Flux and pH-Correlation Curves

### a) Original PS-P4VP Membranes

According to the data statistics, the average flux of P5722 is around 800 L/(h*bar*$m^2$), and that of P3910 is around 600 L/(h*bar*$m^2$).

The pH-correlation curves of the original P3910 membrane are depicted in Fig 3.3.1. The pore size is reduced seriously with pH decreasing, and a significant hysteresis is observed. As discussed in Sec I.2.d, the protons attach to the nitrogen-ends in P4VP tails and this bonding drags the P4VP tail outwards, which forces the pores to close. But at the same time the distance between micelle segments increases and brings in a contractive force. These two competing effects weigh differently in pH-increasing and pH-decreasing curves and result in a gap between them. Hyteresis should be considered carefully when testing each membranes.

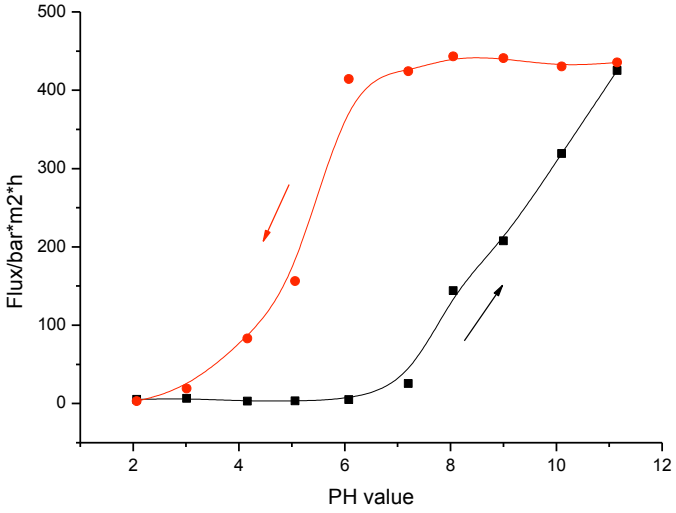


Fig 3.3.1 pH-Correlation Curves for P3910+DDT
Black: pH-increasing curve Red: pH-decreasing curve

**b) Cross-linked PS-P4VP Membranes Induced by 1,4-diiodobutane**

The results for the membranes treated in 1% and 2% 1,4-diiodobutane solution are very close to each other at 500~600 liter/(h*bar*$m^2$), but they are both lower than the original PS-P4VP membranes.

The pH-correlation curves of 1,4-diiodobutane-treated membranes are depicted in Fig 3.3.2 and 3.3.3. The pH-dependence of the pore size is reduced but the hysteresis is not eliminated. 1,4-diiodobutane induces cross-linking between the micelles, which helps to stabilize the microstructure and to fix the distance between cores. Also, the carbon-ends of 1,4-diiodobutane molecules connect to the nitrogen-ends in P4VP tails and prevent them from protonation. Both factors decrease the pH-dependence of pore size and makes the pH-correlation curves "flatter" than orginal membranes.

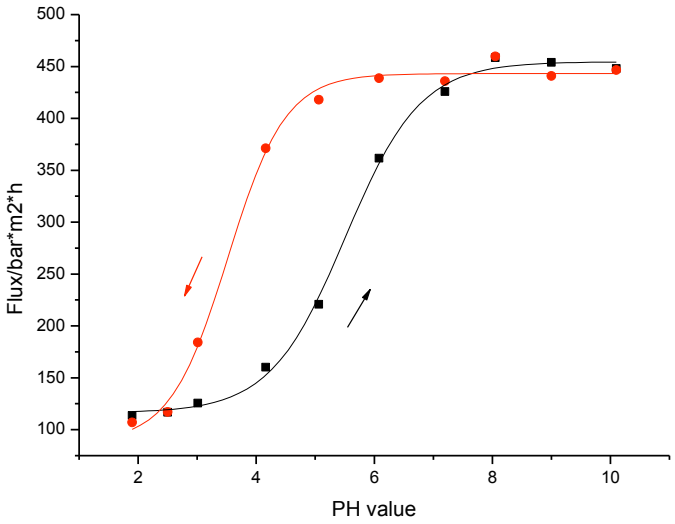


Fig 3.3.2 P3910+DDT +1% 1,4-diiodobutane

Black: pH-increasing curve Red: pH-decreasing curve

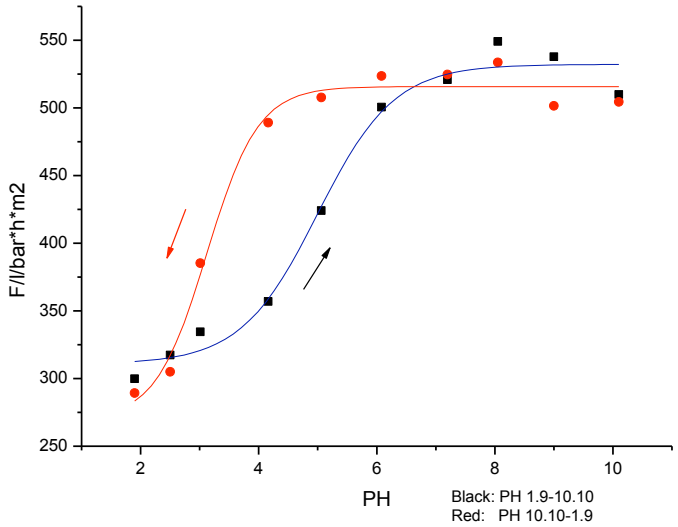


Fig 3.3.3 P3910+DDT+2% 1,4-diiodobutane

Black: pH-increasing curve Red: pH-decreasing curve

The protonation-reducing effect of 1,4-diiodobutane in acid environment is also stronger if the concentration of 1,4-diiodobutane is greater in the solution. Comparing Fig 3.3.2 and 3.3.3 we can see that the flux at a low pH is much higher in 2% 1,4-diiodobutane membrane than in 1% while the flux at a high pH for both concentration is almost the same because the protonation has been relieved.

However, 1,4-diiodobutane changes the microstructure of PS-P4VP isoporous membranes, so the hysteresis is only reduced but not eliminated. And 1,4-diiodobutane-treated membranes are not sensitive to [$H^+$], which is not proper to use in certain environments where protonation is needed.

**c) PS-P4VP-SWCNT Membranes**

The wate flux for different SWCNT concentrations are listed in Table 3.3.1, and they are not very different from the original P3910 membranes, which indicates that SWCNT has not affected the flux much.

The pH-correlation curves of PS-P4VP-SWCNT membranes are depicted in Fig 3.3.4. Water flux returns to normal when the pH is increased back in de-ionized water after an decrease and the two normal pH-correlation curves overlap with each other. In other words, SWCNT has reduced the hysteresis significantly. The length of SWCNT is much greater than the micelle diameter, so each nanotube is able to link with several micelles. This factor additionally stabilizes the assembly structure. When the interaction between nanotubes and micelle cores is strong enough, the intercore distance between two neighboring micelles is not changed when P4VP tails are pronated. In this case only the pore size changes with the pH value and the hysteresis is eliminated. (Gap between the curves vanishes.)

Table 3.3.1 Water Flux of PS-P4VP-SWCNT Membranes with Different SWCNT Concentrations (De-ionized Water, pH~6.2)

| Polymer | Polymer Concentration (%) | SWCNT Concentration (%) | Water Flux [$L/(bar \cdot h \cdot m^2)$] |
|---|---|---|---|
| P5722 | 16.6 | 0.1 | 563.6 |

| | | | |
|---|---|---|---|
| P5722 | 16.6 | 0.2 | 850.5 |
| P5722 | 16.6 | 0.4 | 651.6 |
| P3910 | 20.0 | 0.08 | 420.8 |
| P3910 | 20.0 | 0.16 | 378.5 |
| P3910 | 20.0 | 0.32 | 353.9 |

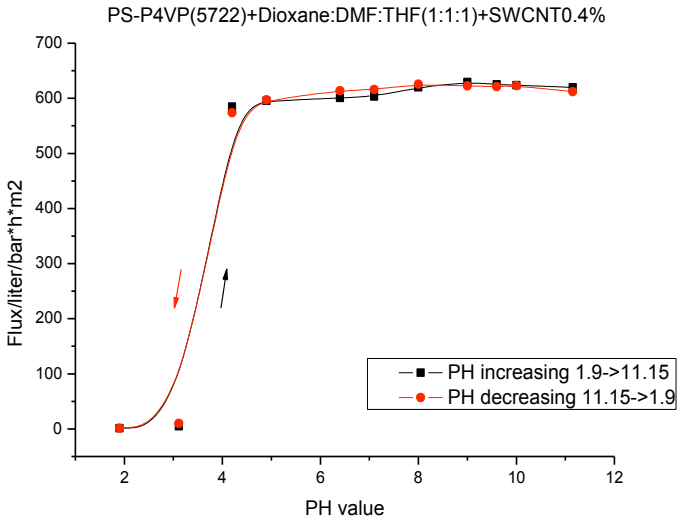


Fig 3.3.4 pH-Correlation Curves for P5722-SWCNT+DDT

Black: pH increasing curve Red: pH decreasing curve

### d) Summary and Discussions

Table 3.3.2~3.3.4 list the comparision of water flux from different membranes. And Fig 3.3.5 and 3.3.6 depict the comparison of pH-increasing and pH-decreasing curves respectively.

Comparing these figures and tables we can see

1) Protonation to the membrane decreases the permeance. This phenomenon becomes stronger when [$H^+$] increases and there is a threshold pH value (5~6 in this research). When pH is higher than this threshold, the permeance does not change much.

2) With pH dropping ([$H^+$] increasing) in an acid solution the pore size

decreases dramatically, and at around pH=1.9 the pores are almost closed. While in a neutral or basic environment the pore size is normal.

3) The flux is very low under high [$H^+$] and it recovers to only 75%-85% of the original value when the environement turns back to neutral or basic. As discussed in Sec I.2.d, $H^+$ protonates on the P4VP tail and makes a strong connection.

4) 1,4-diiodobutane induces cross-linking and decreases the flexibility of pores and micelles. That explains why flux changes of the 1,4-diiodobutanes-treated membranes are much smaller than the original ones.

5) SWCNT increases the stability of pores and micelles, and protects them from being affected by $H^+$. The protection is long-lasting and thus the pore size, the micelle distance and the water flux can be easily recovered when the solution is no longer acid.

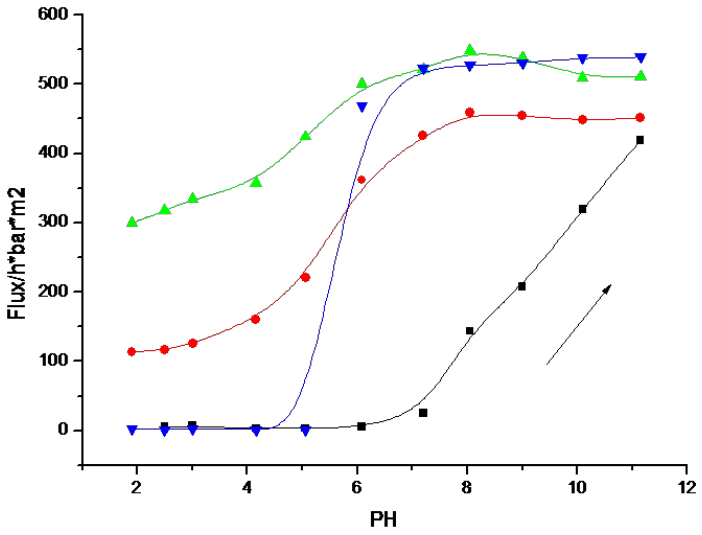


Fig 3.3.5 Comparison of pH increasing curves

Black: Original Red: 1% 1,4-diiodobutane Green: 2% 1,4-diiodobutane Blue: SWCNT

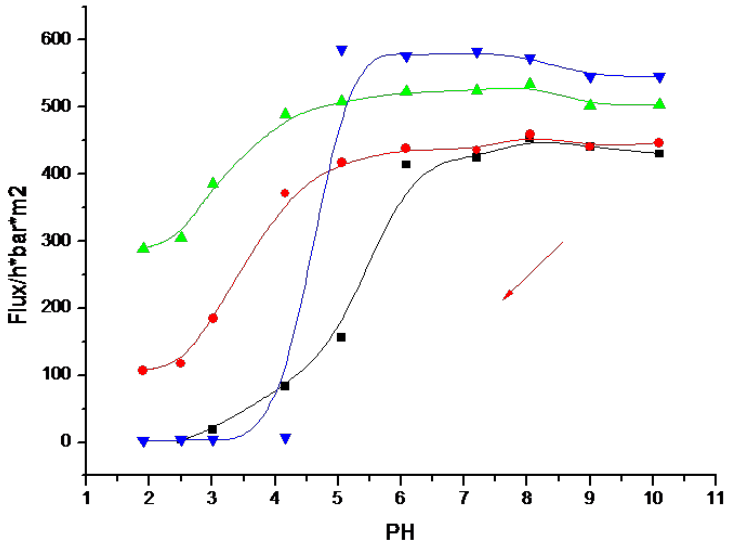


Fig 3.3.6 Comparison of pH decreasing curves

Black: Original Red: 1% 1,4-diiodobutane Green: 2% 1,4-diiodobutane Blue: SWCNT

Table 3.3.2 Effective Climax Flux in pH-Correlation Curve

| P3910 Membranes | Original flux [L/(bar · h · m$^2$)] | Climax flux in pH-increasing curve [L/(bar · h · m$^2$)] | Climax flux in pH-decreasing curve [L/(bar · h · m$^2$)] |
|---|---|---|---|
| Original | 590.8 | 425 (71.94%) | 443 (74.98%) |
| 1% 1,4-diiodobutane | 590.8 | 458 (77.52%) | 459 (90.77%) |
| 2% 1,4-diiodobutane | 606.3 | 549 (90.55%) | 533 (87.91%) |
| SWCNT | 603.7 | 548 (90.77%) | 586 (97.07%) |

Table 3.3.3 Effective Flux Range in pH-increasing Curve

| P3910 Membranes | Original flux [L/(bar · h · m$^2$)] | Climax flux in pH-increasing curve [L/(bar · h · m$^2$)] | Lowest flux in pH-increasing curve [L/(bar · h · m$^2$)] | Flux difference |
|---|---|---|---|---|
| Original | 590.8 | 425 | 3 | 423 (71.59%) |
| 1% 1,4-diiodobutane | 590.8 | 458 | 113 | 345 (58.40%) |
| 2% 1,4-diiodobutane | 606.3 | 549 | 299 | 250 (41.23%) |
| SWCNT | 603.7 | 548 | 2 | 546 (90.44%) |

Table 3.3.4 Effective Flux Range in pH-decreasing Curve

| P3910 Membranes | Original flux | Climax flux in | Lowest flux in | Flux |
|---|---|---|---|---|

| | [L/(bar · h · $m^2$)] | pH-increasing curve [L/(bar · h · $m^2$)] | pH-increasing curve [L/(bar · h · $m^2$)] | difference |
|---|---|---|---|---|
| Original | 590.8 | 443 | 3 | 440 (74.47%) |
| 1% 1,4-diiodobutane | 590.8 | 459 | 106 | 353 (59.75%) |
| 2% 1,4-diiodobutane | 606.3 | 533 | 289 | 244 (40.24%) |
| SWCNT | 603.7 | 586 | 2 | 584 (96.74%) |

## 4. Comparison of Two PS-P4VP Membranes P3910 and P5722

The properties for two polymers P3910 and P5722 are compared in Table 3.4.1 and the pH-correlation curves of two PS-P4VP-SWCNT membranes are depicted in Fig 3.4.1.

The two pairs of pH-correlation curves in Fig 3.4.1 show that the water flux of P5722-SWCNT membrane is greater than P3910-SWCNT, and the hysteresis is only reduced in P3910-SWCNT membrane but completely eliminated in P5722-SWCNT. The possible reasons are listed as follows:

1) The blocks of P5722 are larger than P3910, and so are the micelles and pores. Perhaps the micelle size of P5722 is more compatible to the scale of SWCNT to make a stronger attachment. This explains why the water flux of P5722-SWCNT is greater and why its hysteresis is much weaker.

2) The integration of SWCNT into P5722 is better than P3910. It is possible that SWCNT chains are not homogeneously dispersed into the P3910 membrane, which therefore slightly hinders SWCNT from taking effect.

3) The P3910-SWCNT membrane was prepared very early when the author's casting skill was not as good as now.

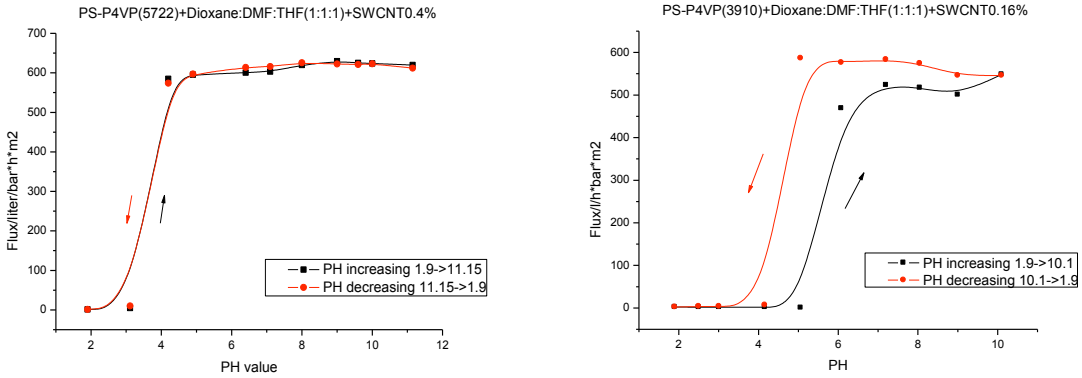


Fig 3.4.1 pH-Correlation Curves for P5722-SWCNT and P3910-SWCNT

Table 3.4.1 Comparison of P5722 and P3910 Membranes

| | P5722 | P3910 |
|---|---|---|
| Solution viscosity | High | Medium |
| Molecular weight ($10^3$ g/mol) | 138-b-41.0 (High) | 109-b-30.0 (Low) |
| Concentration (%) | 16.6% (Low) | 20.0% (High) |
| PS-P4VP-SWCNT | Very well-ordered | Less well-ordered |
| Pore size diameter | ~30nm, a bit greater than P3910 | ~30nm |
| pH-correlation curve | S-shape, high-dependence of $[H^+]$, long reaction time | S-shape, low-dependence of $[H^+]$, flexible, easy to recover |
| Water flux [L/(bar*h*$m^2$)] | ~800 | ~600 |
| (PS-P4VP)-(homo-P4VP) | Very rough and bumpy surface<br>No well-ordered self-assembly<br>Expanded pore size | Less rough and bumpy surface<br>No well-ordered self-assembly<br>Expanded pore size |
| (PS-P4VP)-(homo-P4VP) -SWCNT | Self-assembly structure improved by SWCNT but still not as good as the original PS-P4VP membranes, homo-P4VP not a good additive | |

## 5. Further Discussion of Pore Size Change in Acid Environment

As discussed in Sec I.2.d, the pore size varies in different pH values and results in the different water/gas flux. The relations of gas flux and pore size can be expressed using Hagen-Poiseuille equation.

$$Q = \frac{\varepsilon r^2 \Delta p}{8\gamma l} \quad \text{(Eqn 3.5.1)}$$

Q is gas flux, ε is porosity, r is pore radius, Δp is the pressure difference between feed and permeate, γ is viscosity and l is membrane thickness.

Fig 3.5.1 and 3.5.2 are the AFM images of the original PS-P4VP membrane and the same one after treatment using pH=1 HCl for 1h.

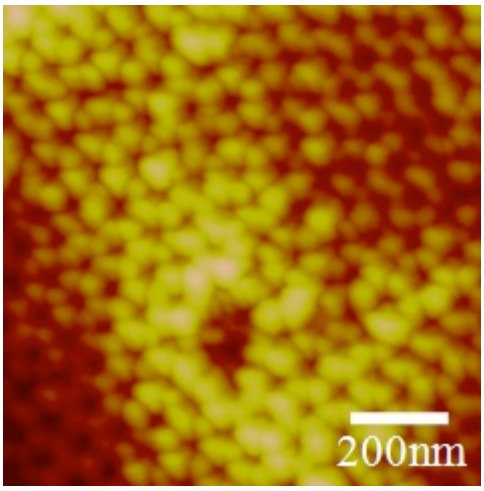


Fig 3.5.1 P5722 Original (Height Sensor)

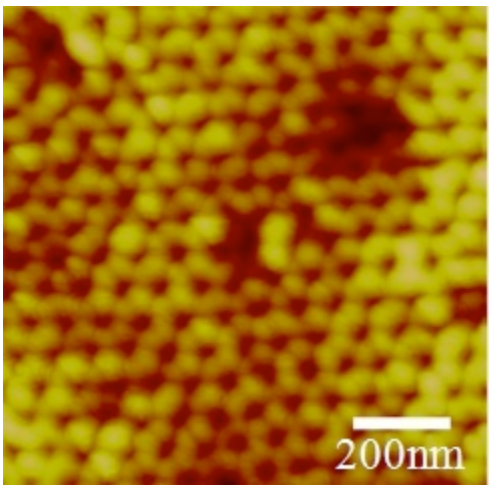


Fig 3.5.2 P5722+HCl for 1h(Height Sensor)

According to the data analysis by Nanoscope Software (Veeco Dimension Icon Atomic Force Microscope), the distance between two neighboring PS-P4VP micelles is 35 nm in Fig 3.5.1 and 25 nm in Fig 3.1.2. Assuming that pore radius is the only variable that changes, the gas flux ratio can be obtained theoretically:

$$\frac{Q_1}{Q_2} = \frac{\left(\frac{\varepsilon r_1^2 \Delta p}{8\eta \mathrm{l}}\right)}{\left(\frac{\varepsilon r_2^2 \Delta p}{8\eta \mathrm{l}}\right)} = \left(\frac{r_1}{r_2}\right)^2 = \left(\frac{35}{25}\right)^2 \cong 1.96$$

The gas flux ratios for $N_2$ and $CO_2$ from the experimetal results are

$$\left(\frac{Q_1}{Q_2}\right)_{N_2} = \frac{102.2}{49.6} \cong 2.06 \quad \text{and} \quad \left(\frac{Q_1}{Q_2}\right)_{CO_2} = \frac{80.6}{41.4} \cong 1.95$$

Both values agree well to the theoretical result and thus the Hagen-Poiseuille equation works well for the PS-P4VP polymer membrane.

P3910 membranes were not used in this part of experiment because their surface structures were not as good as P5722 membranes, and the P3910 copolymer was out of stock.

# Chapter IV

# CONCLUSIONS

This thesis research work focused on PS-P4VP isoporous membranes used for water filtration and gas permeation, and can be concluded in the following:

1. Two PS-P4VP polymer materials P5722 and P3910 were chosen in the polymer screening using mixing solvent DDT (DOX+DMF+THF), because they produced isoporous structure and well-ordered surface as desired in mass separation;

2. PS-P4VP membranes were prepared using casting method and four additives (1,4-diiodobutane, homo-P4VP, SWCNT and $Cu(Ac)_2$) were used based on the analysis. All the isoporous self-assembly structures of these membranes were observed using AFM and their water/gas flux and hysteresis were compared with each other using pH-correlation curves.

3. Pore size was found a key variable determining the water/gas flux that could be reduced during to the protonation of the P4VP tails. And Hagen-Poiseuille equation was proved to express the relations between the pore radius and the gas flux well.

4. Hysteresis was a significant phenomena in the form of a great gap between pH-increasing and pH-decreasing curves. This was because the two results of P4VP

protonation – the shut-down/open of pores and the increase/decrease of micelle distance – acted in different ways in pH-increasing and pH-decreasing process. Hysteresis can be reduced or even eliminated by additives 1,4-diiodobutane and SWCNT.

5. 1,4-diiodobutane was used as the cross-linking inducer. The cross-linked membranes were proved to have a smaller water flux (as the pore size was reduced) and a less serious hysteresis (as the micelle and the distance between the cores were partially fixed). The 2% 1,4-diiodobutane membrane had a higher water flux at a low pH than the 1% 1,4-diiodobutane membrane.

6. Homo-P4VP was used as an additive to enlarge the pore size. But it was found to have disturbed the micelle structure and made the surface uneven.

7. Two enhancements of SWCNT were observed to the membranes. a) The membrane structure became more ordered and more appropriate for aqueous separation. b) Hysteresis was significantly decreased because SWCNT stabilized the membrane structure and fixed the distance between the cores. It was a pity that the effect of SWCNT concentration was not thoroughly explored when the polymer materials got out of stock.

8. $Cu(Ac)_2$ was used as a substitute of DOX in DDT solvent (and formed CDT solvent) for a better dispersion of SWCNT in the solution. But membrane qualities were not yet satisfactory enough.

Based on these research works the author believes PS-P4VP is a good

copolymer material for making isoporous membranes and the membrane quality can be improved by some other additives, such as halides and SWCNT.

What deserves to be mentioned here is that SWCNT was a very important finding in this research. SWCNT was proved to possess many beneficial factors for membranes, though there were not many groups discussing it until recently. In this research the author detected some of the advantages but the progress was limited by the little stock of polymers. However, the author still believes SWCNT added into isoporous membranes is a future subject of significance.

# BIBLIOGRAPHY

(1) Bernardo, P.; Drioli, E.; Golemme, G. *Industrial & Engineering Chemistry Research* **2009**, *48*, 4638.

(2) Koros, B. *Journal of Membrane Science* **2007**, *300*, 1.

(3) Baker, R. W. *Industrial & Engineering Chemistry Research* **2002**, *41*, 1393.

(4) Montgomery, M. A.&Elimelech, M. *Environ. Sci. Technol.***2007**, 41, 17-24.

(5) Molinari, R.; Palmisano, L.; Drioli, E.; Schiavello, M. *Journal of Membrane Science* **2002**, *206*, 399.

(6) Shannon, M. A.; Bohn, P. W.; Elimelech, M.; Georgiadis, J. G.; Mariñas, B. J.; Mayes, A. M. *Nature* **2008**, *452*, 301.

(7) Caetano, A. *Membrane technology: applications to industrial wastewater treatment*; Springer, **1995**.

(8) Pramauro, E.; Bianco Prevot, A. *Pure and applied chemistry* **1995**, *67*, 551.

(9) Ho, W. S. W.; Sirkar, K. K. *Membrane Handbook; Van Nostrand Reinhold*: New York, **1992**.

(10) Baker, R. W. *Membrane Technology and Applications*, 2nd ed.; John Wiley: New York, **2004**.

(11) Geise, G. M.; Lee, H. S.; Miller, D. J.; Freeman, B. D.; McGrath, J. E.; Paul, D. R. *Journal of Polymer Science Part B: Polymer Physics* **2010**, *48*, 1685.

(12) Baker, R. W. *Industrial & Engineering Chemistry Research* **2002**, *41*, 1393.

(13) Hashemipoor, N.; PS-P4VP chemical structure, © ***2010*** *Polymer Source Inc*. Retrieved May 25th, 2011, from http://www.polymersource.com/productSearch.php?ID=P3910A-S4VP

(14) Peinemann, K. V.; Abetz, V.; Simon, P. F. W. *Nature materials* **2007**, *6*, 992.

(15) Nunes, S. P.; Sougrat, R.; Hooghan, B.; Anjum, D. H.; Behzad, A. R.; Zhao, L.; Pradeep, N.; Pinnau, I.; Vainio, U.; Peinemann, K. V. *Macromolecules* **2010**.

(16) Hamley, I. *Nanotechnology* **2003**, *14*, R39.

(17) Park, S.; Wang, J. Y.; Kim, B.; Xu, J.; Russell, T. P. *ACS nano* **2008**, *2*, 766.

(18) Serghei, A.; Zhao, W.; Wei, X.; Chen, D.; Russell, T. *The European Physical Journal-Special Topics* **2010**, *189*, 95.

(19) Sohn, B.; Seo, B. *Chemistry of materials* **2001**, *13*, 1752.

(20) Yun, S. H.; Sohn, B. H.; Jung, J. C.; Zin, W. C.; Lee, J. K.; Song, O. *Langmuir* **2005**, *21*, 6548.

(21) Yun, S. H.; Yoo, S. I.; Jung, J. C.; Zin, W. C.; Sohn, B. H. *Chemistry of materials* **2006**, *18*, 5646.

(22) Ma, G.; Fukutomi, T. *Macromolecules* **1992**, *25*, 1870.

(23) Saito, R.; Fujita, A.; Ichimura, A.; Ishizu, K. *Journal of Polymer Science Part A: Polymer Chemistry* **2000**, *38*, 2091.

(24) Saito, R. *Macromolecules* **2001**, *34*, 4299.

(25) Hashemipoor, N.; Homo P4VP chemical structure, © ***2010*** *Polymer Source Inc*. Retrieved May 25th, 2011, from

http://www.polymersource.com/productSearch.php?ID=P130-4VP

(26) Cong, Y.; Zhang, Z.; Fu, J.; Li, J.; Han, Y. *Polymer* **2005**, *46*, 5377.

(27) Han CC, Mozer B. *Macromolecules* **1977**;10:44..

(28) Special issue on Carbon Nanotubes. *Acc. Chem. Res.* **2002**, *35*, 997.

(29) Star, A.; Han, T. R.; Joshi, V.; Gruner, G. *POLYMER PREPRINTS-AMERICA*- **2003**, *44*, 201.

(30) Nunes, S. P., Peinemann, K.-V., *et al. Langmuir*; **2011** (submitted)

(31) Graphite-like Structure of Single-Wall Carbon Nanotube (SWCNT), © ***2011*** *The Trustees of Boston College.* Retrieved May 25th, 2011, from http://t2.gstatic.com/images?q=tbn:ANd9GcTd72c3iAhqhka WKmVTCPwTntApTimpa_79PgsAKk67F_bblG4R&t=1

(32) Microscopic Image of Single-Wall Carbon Nanotube (SWCNT), © ***2011*** *First Nano.* Retrieved May 25th, 2011, from http://www.firstnano.com/img/photos/applications1.jpg

(33) Belfiore, L.; McCurdie, M. P. *J. Polym. Sci.*, *Part B: Polym. Phys.* **1995**, 33, 105-124.

(34) Israelachvili, J. N., *Intermolecular and Surface Forces. 9th ed., Elsevier Science Imprint:* London, **2002**, 450.

(35) Nagarajan, R., *Langmuir*, **2002,** *18,* 31-38

(36) Binnig, G., Quate, C. F., *Phys. Rev. Let.*, **1986**, 56(9), 930-933

(37) Giessibl, F. J. , *Rev. Mod. Phys.*, **2003**, 75: 949.